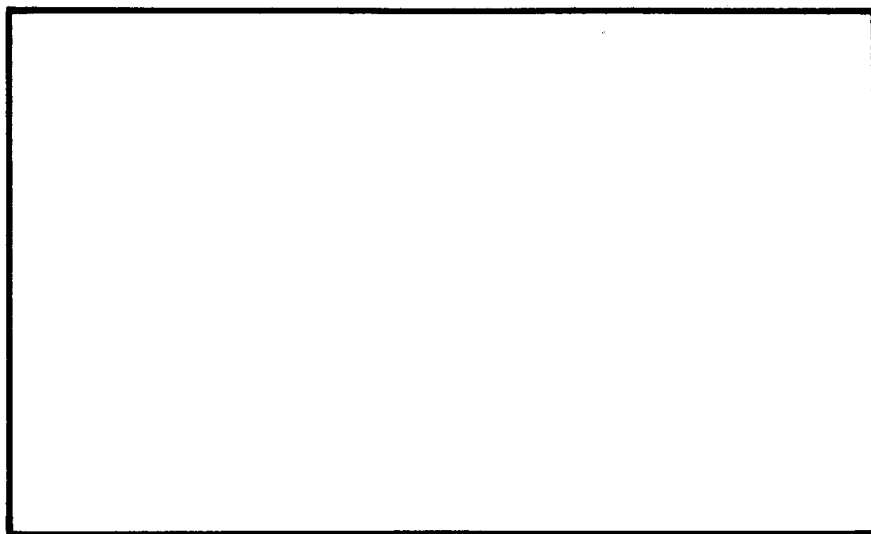
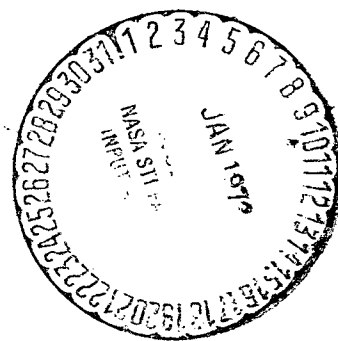


1-8

CR-130133



FAIRCHILD
REPUBLIC DIVISION



(NASA-CR-130133) PULSED PLASMA SOLID
PROPELLANT MICROTHRUSTER FOR THE
SYNCHRONOUS METEOROLOGICAL SATELLITE
TASK W.J. Guman (Fairchild Industries,
Inc.) Aug. 1972 63 p CSCL 21C

N73-14794

Unclas
G3/28 51286

NTIS \$5.25

FRD 4090
August 1972

TASK 4 - ENGINEERING MODEL FABRICATION
AND TEST REPORT

Pulsed Plasma Solid Propellant Microthruster
for the Synchronous Meteorological Satellite
Interim Report for Period April 1972-July 1972

FAIRCHILD

Fairchild Republic Division Farmingdale, New York 11735

FRD 4090
August 1972

TASK 4 - ENGINEERING MODEL FABRICATION AND TEST REPORT

Pulsed Plasma Solid Propellant Microthruster for the Synchronous
Meteorological Satellite

Edited by: William J. Guman
Fairchild Industries
Fairchild Republic Division
Farmingdale, New York 11735

August 1972

Interim Report for Period April 1972 - July 1972

Prepared for

GODDARD SPACE FLIGHT CENTER
Greenbelt, Maryland 20771

TECHNICAL REPORT STANDARD TITLE PAGE

1. Report No.		2. Government Accession No.		3. Recipient's Catalog No.	
4. Title and Subtitle TASK 4 - ENGINEERING MODEL FABRICATION AND TEST REPORT				5. Report Date August 1972	
				6. Performing Organization Code	
7. Author(s) Edited by W. J. Guman				8. Performing Organization Report No. FRD 4090	
9. Performing Organization Name and Address Fairchild Industries Fairchild Republic Division Farmingdale, New York 11735				10. Work Unit No.	
				11. Contract or Grant No. NAS5-11494	
12. Sponsoring Agency Name and Address Goddard Space Flight Center Greenbelt Maryland 20771 Mr. T. E. Williams				13. Type of Report and Period Covered Interim Task Report April 1972-July 1972	
				14. Sponsoring Agency Code	
15. Supplementary Notes					
16. Abstract <p>Two flight prototype solid propellant pulsed plasma microthruster propulsion systems for the SMS satellite were fabricated, assembled and tested. The propulsion system is a completely self contained system requiring only three electrical inputs to operate: a 29.4 volt power source, a 28 volt enable signal and a 50 millsec long command fire signal that can be applied at any rate from 50 ppm to 110 ppm. The thrust level can be varied over a range 2.2 to 1 at constant impulse bit amplitude. By controlling the duration of the 28 volt enable signal either steady state thrust or a series of discrete impulse bits can be generated. A new technique of capacitor charging has been implemented to reduce high voltage stress on energy storage capacitors.</p>					
17. Key Words (Selected by Author(s)) Electric Propulsion Pulsed Plasma Thrusters Satellite Control Plasma Propulsion				18. Distribution Statement	
19. Security Classif. (of this report) Unclassified		20. Security Classif. (of this page) Unclassified		21. No. of Pages	
				22. Price* 5.25	

*For sale by the Clearinghouse for Federal Scientific and Technical Information, Springfield, Virginia 22151.

CONTENTS

<u>Section</u>		<u>Page</u>
1.0	INTRODUCTION	1
2.0	FABRICATION AND FINAL ASSEMBLY	2
2.1	Delivery Experience	2
2.2	Fabrication Experience	2
2.3	System Assembly	6
2.3.1	In-Process Testing	6
2.3.2	Thermistor Calibration	6
2.3.3	Torques	11
2.3.4	Integration of Power Conditioning Subassembly	11
2.4	System Weight, CG Location	13
2.5	Mounting Hole Pattern, Thrust Axis Location	16
2.6	Connector Location	16
3.0	SYSTEM OPERATION	19
3.1	General	19
3.2	On the Satellite	21
3.3	In the Laboratory	21
3.4	System Shutdown	22
3.4.1	On a Spacecraft	22
3.4.2	In the Laboratory	22
3.5	Power Conditioning Subsystem Operation	22
4.0	TESTING CARRIED OUT	24
4.1	Power Conditioning Test Data	24
4.1.1	By the Vendor	24
4.1.2	Prior to Integration	33
4.1.3	Input Current Measurements	34
4.1.4	Total Propulsion System Power Measurements	40
4.1.5	Time Average Power of Charge Cycle	41
4.2	Performance Acceptance Tests	44
4.2.1	Thrust and Impulse Bit Data	46
4.2.2	Total Impulse Capability	46
4.2.3	Measured High Voltage Output	51
5.0	FINAL REMARKS	54
6.0	REFERENCES	55

ILLUSTRATIONS

<u>Figure</u>		<u>Page</u>
1	Solid Propellant Pulsed Plasma Microthruster System	5
2	Microthruster System with Exterior Housing and Exhaust Cone Removed	7
3	Microthruster System Showing Exterior Location of Integrated Power Conditioning Subsystem	12
4	Thruster Electronics Subassembly	14
5	Location of CG and Mounting Holes	15
6	Front View of Propulsion System	17
7	Side View of System Showing Connector Location	18
8	Interior View of Power Conditioning Subsystem	25
9	Input Current at 108 ppm	38
10	Input Current at 85.3 ppm	38
11	Input Current at 70 ppm	39
12	Input Current at 53.5 ppm	39
13	Time Average System Power Consumption	42
14	High Voltage Output at 104.5 ppm	52
15	High Voltage Output at 83 ppm	52
16	High Voltage Output at 69 ppm	53
17	High Voltage Output at 53.8 ppm	53

<u>Table</u>		<u>Page</u>
1	Delivery Experience	3
2	In-Process Tests Performed	8
3	Thermistor Calibration Data	9
4	Thermistor Calibration Data	10
5	Connector Pin Assignment	19
6	Steady State Output Data - Unit No. 1	26
7	Output Data as a Function of Input Voltage Variation	26
8	Data with Resistive Load	27
9	Short Circuit Data	27

ILLUSTRATIONS (Cont'd)

<u>Table</u>		<u>Page</u>
10	Telemetry Calibration Data (Steady State)	29
11	Steady State Output Data - Unit No. 2	30
12	Output Data as a Function of Input Voltage Variation	30
13	Data with Resistive Load	31
14	Short Circuit Data	31
15	Telemetry Calibration Data (Steady State)	33
16	Charge and Hold Time for Power Conditioner No. 1	35
17	Charge and Hold Time for Power Conditioner No. 2	36
18	Time Average Current of Complete Propulsion System	37
19	Time Average Power of Complete Propulsion System	40
20	Time Average Power Averaged Over the Capacitor Charge Cycle	41
21	Comparison of Actual to Ideal Total System Power (Thruster B)	43
22	Performance Acceptance Tests	44
23	Thrust and Impulse Bit Data Log 146-1, 146-3	47
24	Acceptance Thrust and Impulse Bit Data System 1, (Log 146-4)	48
25	Acceptance Thrust and Impulse Bit Data System 2, (Log 147-1)	49
26	Impulse Bit Amplitude Variation	50

PREFACE

This report presents the results of the final task of the program. The work described covers the experience and results of fabricating, assembling and testing the flight prototype pulsed plasma microthruster propulsion system for the SMS application. Many individuals contributed to the efforts described in this report. Mr. J. Chung performed the final design of the system with invaluable contributions provided by Mr. M. Katchmar. Messrs. R. Gelbman and J. McIver participated in electrical subassembly tests. The laboratory effort was supervised by Mr. L. Brown with efforts carried out by Messrs. M. Katchmar, H. Lubben, A. Scheiwiller and J. Pokorny. The power conditioning subassembly was fabricated and tested at Wilmore Electronics, Inc., under the direction of Dr. E.T. Moore. The program was directed by the principal investigator Dr. W.J. Guman at Fairchild Republic with Mr. T.E. Williams being the NASA Goddard Space Flight Center Technical Officer.

Even though some problems were encountered during this last task of the program, these were resolved and the final results have successfully transformed the analysis and design effort of the earlier tasks into operational hardware. The two flight prototype propulsion systems that were fabricated, assembled and tested met all expectations and demonstrated that the SMS mission propulsive performance requirements can be met.

1.0 INTRODUCTION

This Task 4 report discusses fabrication, assembly and testing of the solid propellant pulsed plasma microthruster system for the SMS satellite. References 1 and 2 presented details of the analysis and design of the propulsion system, respectively.

The final system hardware and performance is as originally envisioned and proposed. The complete propulsion system is a completely self-contained package consisting of all of the subsystems necessary to functionally operate the propulsion system in the simplest possible manner over a pulse frequency range which can vary from 50 ppm to 110 ppm (i.e., a 2.2 to 1 steady thrust level variation at constant specific impulse and thrust efficiency). Indeed, besides the inherent simplicity of the basic thruster concept, overall system operation is equally extremely simple. System operation requires only three inputs:

1. A 29.4 ± 0.2 VDC primary power input
2. A 28 ± 2 VDC enable signal input
3. A 50 millsec ± 5 ms long, 5 ± 0.5 V amplitude command fire signal input provided at any desired pulse rate in the range from 50 ppm to 110 ppm to produce either a train of impulse bits or an equivalent steady state thrust level.

Both the 29.4 volt primary power and the 50 millisec long command fire signal inputs can be impressed continuously upon the propulsion system. Without drawing power, the system will be "off" until the 28 volt enable signal is applied. Upon application of the 28 volt enable signal the system will draw power and process the fire command signal. Depending upon the rate of the applied command fire signal, the first impulse bit will be provided in the range from 0.55 sec to 1.2 seconds after enabling the system. Removal of the 28 volt enable signal instantly shuts down the system without further power being drawn from the primary power source.

Mechanical and electrical integration of the system to the SMS satellite is equally simple. Only one electrical connector is required to perform electrical integration of the propulsion system and three hold-down bolts mechanically interface the entire system to the spacecraft.

The concept of significantly reducing the hours of applied high voltage on the thruster capacitor⁽¹⁾ has been incorporated into the power conditioner design and shown

to be feasible. This new technique of capacitor charging for the variable pulse rate (50 ppm to 110 ppm) mission of the SMS satellite will significantly reduce the high voltage stress of the energy storage capacitor and extend capacitor life in cases when system operation will be at lower pulse rates than maximum pulse rate capability.

The complete propulsion system falls within the envelope as presented in NASA GSFC Drawing GC1171302.

The final acceptance performance data of both systems that were assembled and tested have met the impulse bit amplitude requirement and sufficient propellant is provided to exceed the 400 lb-sec requirement. Propulsive performance and system weight of the two systems are virtually identical showing that these latter aspects are indeed reproducible as has also been previously demonstrated in the LES-6 program⁽³⁾. Furthermore, the system of this program demonstrates that the flight proven LES-6 concept can be scaled to a higher level of performance capability.

Some problems were encountered during fabrication, assembly and testing. While they were not major problems, they did require time and effort to resolve. However, the problem of vendors meeting delivery schedules may reoccur. By hindsight it is now also possible to see some areas for future improvements which would simplify fabrication and also facilitate assembly of the complete system.

2.0 FABRICATION AND FINAL ASSEMBLY

2.1 Delivery Experience

While most of the electronic components required in the system could be selected from NASA PPL-11 a few items were nonstandard. Specifications for their procurement, which also includes the screening to be performed by the vendor, were issued for these nonstandard parts. Almost invariably extremely long delivery schedules were encountered in obtaining these nonstandard screened parts. Some representative data is presented in Table 1 illustrating the time lapse from the time the purchase order was issued and the time the item was available for installation. An extremely long delay was encountered in procuring Silicon Controlled Rectifiers from General Electric. After 23 weeks only a high reliability version of the SCR was made available to us. While these had been screened by the vendor to his specification, they still had not been screened to our more stringent specification. Units screened to our specification arrived at Republic too late to be installed

TABLE 1. DELIVERY EXPERIENCE

<u>Item</u>	<u>Specification</u>	<u>Elapsed Time From Purchase Until Available*</u>
Energy storage capacitor	PC145S8001	22 weeks
SCR (high reliability)	PC145S8004	23 weeks ("unscreened")
Diode	PC145S8006	19 weeks
Pulse transformer	PC145S8007	19 weeks
Negator spring coating	PC145S8009	17 weeks

* This time also includes incoming receiving inspection.

in the two flight prototype thrusters. In order not to delay delivery of the systems significantly, it became necessary to perform the additional screening at Republic. Mykroy insulating material turned out also to have an extremely long delivery schedule. Due to a fire in the vendor's plant, a delivery date of up to one year was quoted.

The delivery schedules encountered with the items presented in Table 1 generally exceeded quoted schedules and also the delivery schedules previously encountered with the vendor. Fortunately, previous experience with these components had tagged most of these items as long lead items. The longer than promised delivery delay encountered with some of these items would have caused a final delivery slippage, if the program itself had not slipped in the interim. The experience gained during this program suggests that in future programs the above long lead items should be placed on order immediately upon inception of the program.

2.2 Fabrication Experience

In an attempt to reduce system weight to an absolute minimum, the design approach taken was to eliminate any unnecessary material not absolutely essential to system structural integrity. Considerable machining operations were, therefore, called for to comply with the design requirements. Furthermore, extremely close tolerances were called for to facilitate interchangeability of parts and to assure proper fitting of all interfacing parts. While extreme care was required, no major problems

were encountered during fabrication of machined parts. Problems were encountered, however, in the manufacture of the exhaust cone (PC145D1080). During fabrication it was required to weld the 0.020 in. thick aluminum exhaust cone surface to a 0.090 in. thick aluminum mounting flange (see Figure 1). Subsequently this welded assembly had to be heat treated yet maintaining extremely close tolerances of the final product. The substantial difference in thickness of the two pieces to be welded and the fact that they intersected each other at an angle (see Figure 1) where they were to be welded, required more than one unit be made before one was acceptable. A total of 8 weeks elapsed before two acceptable cones were received from the vendor. It has been recommended by the vendor that the 0.020 in. thick aluminum be increased to at least 0.030 inches. Insufficient time was available to perform a redesign of the cone assembly to incorporate the recommended change.

Another problem area encountered occurred during application of Electro-film 2306 dry film lubricant to the Negator spring which feeds the propellant rod. The first delivery was rejected because of poor adherence of the dry film lubricant to the spring surface. The vendor's procedure was carefully reviewed and a new procedure (Fairchild Republic Specification PC145S8009 Rev. A) was developed which provided an acceptable product. The total turn-around time (see Table 1) from issuing the procurement until the final acceptable product was received was 17 weeks. This procurement time would be reduced substantially in future procurements.

The basic thruster subsystem is fastened by means of 8 isolated studs (PC145D1017-1) to the rear bulkhead (PC145D1015) as shown in Figure 5 of Ref. 2. During fabrication it was found that extreme care had to be exercised as these studs were pressed into the bulkhead. Cold flow of the aluminum bulkhead had to be very carefully controlled to maintain the required final tolerances between studs. It is now believed that recessed screws could have been used instead of the studs to simplify fabrication of this part of the bulkhead subassembly.

The RTH06BS472J thermistor used to monitor capacitor case temperature is fabricated in an essentially pellet configuration. It has subsequently been learned from the vendor that it would have been possible to obtain a special molding of the thermistor whose shape would conform more favorably to the cylindrical surface to which it gets attached. This modified configuration would enhance adherence and also increase the thermal contact area between the thermistor and the capacitor case. While no problems

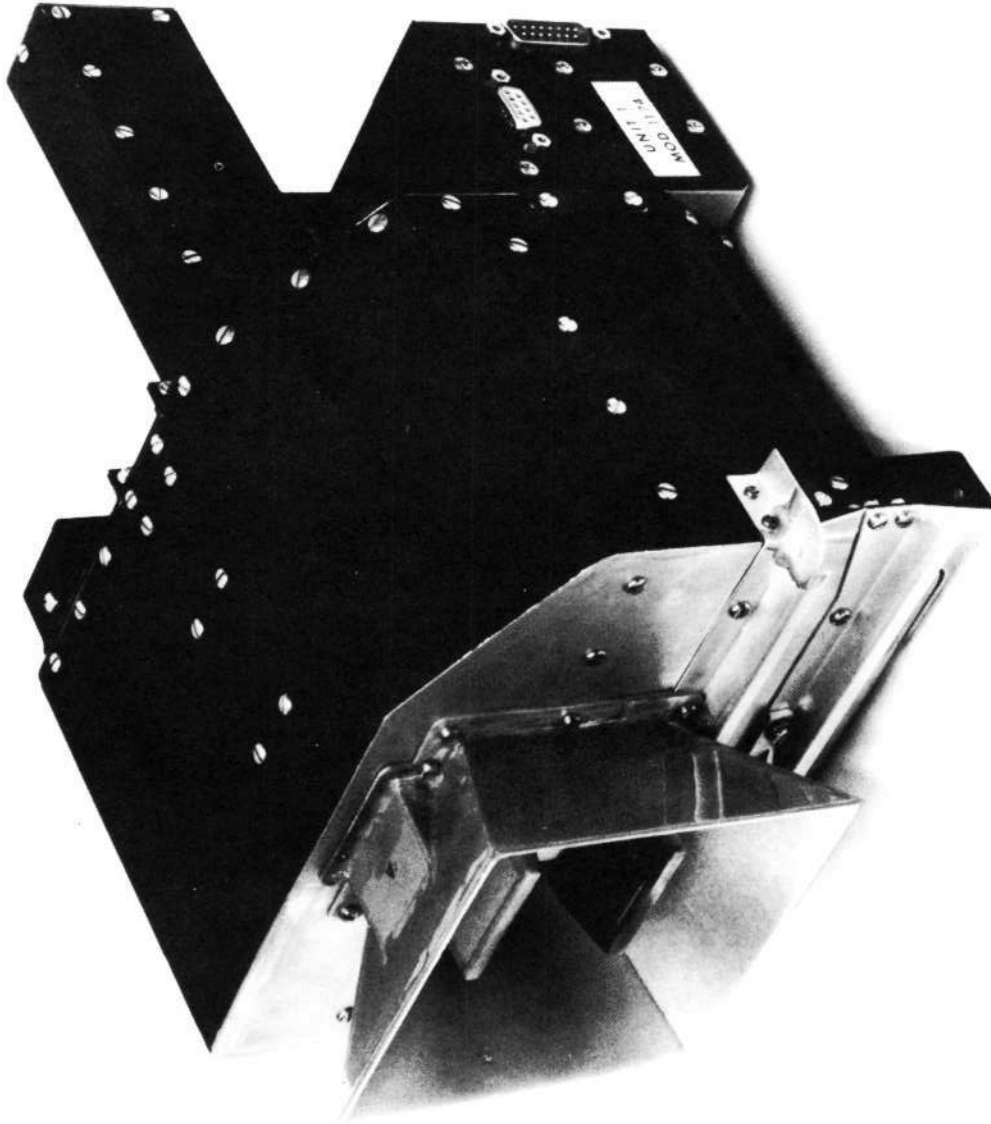


Figure 1. Solid Propellant Pulsed Plasma Microthruster System

were encountered with either adherence or temperature response, it is believed that a specially contoured thermistor would appear more aesthetic.

2.3 System Assembly

For assembly purposes the complete system may be considered to be comprised of three major subassemblies:

- 1) The basic thruster subassembly
- 2) The thruster electronics subassembly
- 3) The power conditioning subassembly

These three major subassemblies are seen by removing the exterior housing and exhaust cone such as shown in Figure 2. Each of these major subsystems can be assembled and functionally checked independent of the other. The function and a description of these subsystems were presented in Refs. 1 and 2. Functional engineering models of each of these subassemblies were fabricated and evaluated during Task 1 of the program. Integration of final versions of these three subassemblies occurred for the first time during the Task 4 effort being reported upon.

2.3.1 In-Process Testing

To assure quality, a series of in-process tests were performed of components of each of the three major subassemblies. Table 2 presents a tabulation of the in-process tests that were performed. These tests are performed in addition to the screening tests on individual electronic parts.

2.3.2 Thermistor Calibration

Capacitor case temperature is monitored by a thermistor. The thermistor output is processed in the power conditioner to provide a 0 to 5 volt telemetry output signal over the temperature range -5°F to $+150^{\circ}\text{F}$. Each thermistor was calibrated with the particular power conditioner to which it interfaces in the final deliverable system. Tables 3 and 4 present the calibration data for thermistors No. 1 and No. 2, respectively.

The thermistor voltage divider circuitry was designed to compromise between using a minimum number of parts, drawing minimum power and to try to get a reasonably good temperature resolution above room temperature when the rate of change of output voltage with change in temperature is smaller than in the low temperature regime. Under worse case conditions, it is possible to determine capacitor case

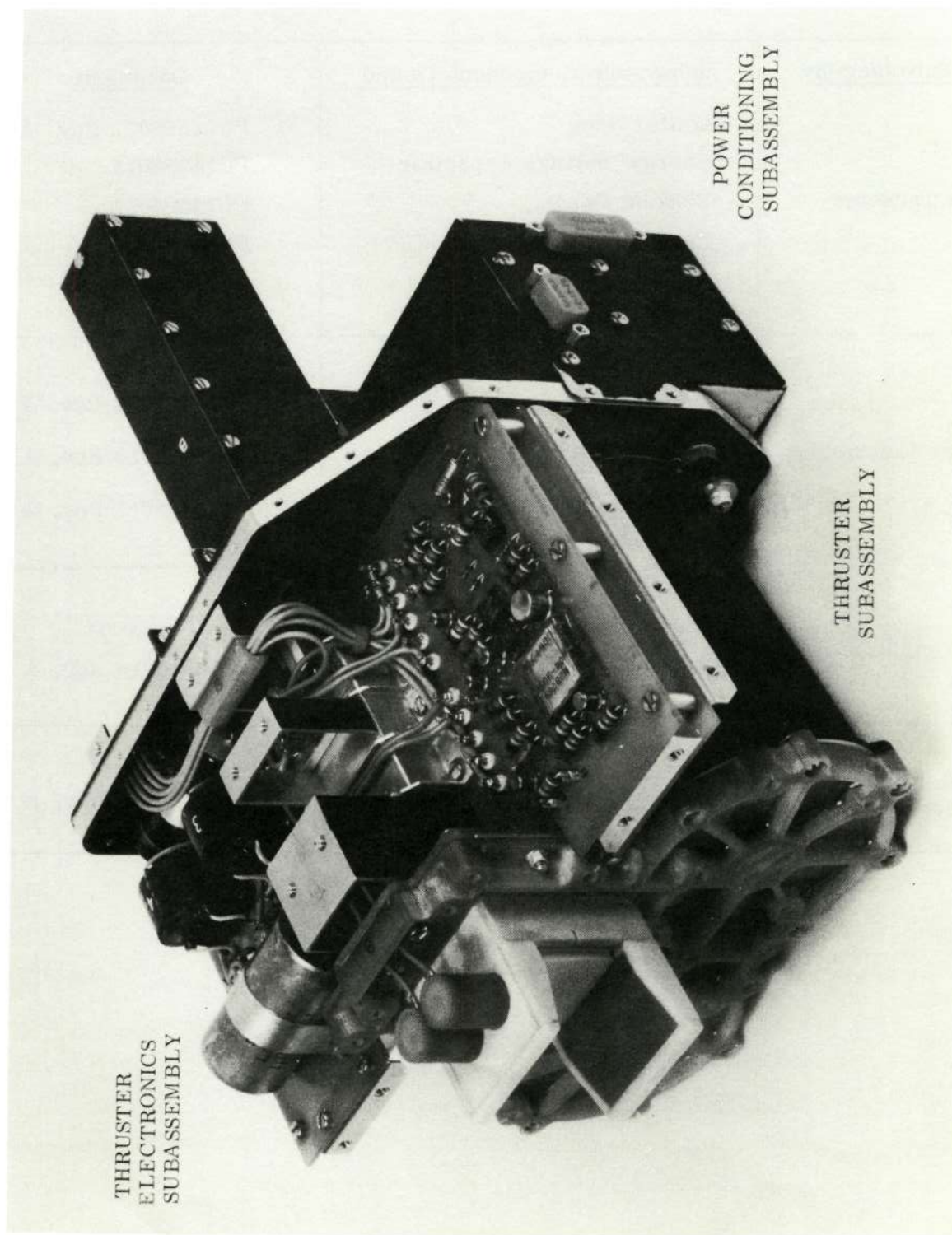


Figure 2. Microthruster System With Exterior Housing and Exhaust Cone Removed

TABLE 2. IN-PROCESS TESTS PERFORMED

<u>Major Subassembly</u>	<u>Subsystem Component Tested</u>	<u>Document</u>
Basic Thruster	Igniter Plug Energy Storage Capacitor Exhaust Cone Face Plate Subassembly PEM Nut Insulation	PC145S8012 Rev. A PC145S8013 PC145S8014 PC145S8019 PC145S8021
Thruster Electronics	Pulse Driver Board Delay Pulse Generator and Flip-Flop Board Discharge Initiating Board	PC145S8015 Rev. A PC145S8016 Rev. A PC145S8017 Rev. A
Power Conditioning	Vendors' Testing Complete System	(Final Report) PC145S8018 Rev. A
Completely Integrated Propulsion System		PC145S8026 Rev. B

TABLE 3. THERMISTOR CALIBRATION DATA

Thermistor Serial Number: 1

Power Conditioner Serial Number: 1

Thermocouple Readout Leeds & Northrup Millivolts	Thermistor Readout Fluke Meter Voltage	Temperature (°F)
-1.02	4.752	-5
- .90	4.600	0
- .79	4.41	3.5
- .70	4.20	7.0
- .56	3.97	12.2
- .42	3.81	15
- .34	3.59	20
- .18	3.27	26
- .18	3.04	32
+ .08	2.86	35
+ .25	2.65	41
+ .37	2.46	45.5
+ .53	2.26	51
+ .67	2.12	56
+ .79	1.93	60
+ .94	1.80	65
+ .99	1.74	67
+1.19	1.55	74
+1.36	1.40	80
+1.51	1.30	85
+1.68	1.15	91
+1.83	1.08	96
+2.00	.96	102
+2.17	.90	108
+2.35	.85	114
+2.52	.75	120
+2.69	.70	126
+2.88	.63	132
+3.11	.58	140
+3.26	.52	145
+3.41	.45	150

TABLE 4. THERMISTOR CALIBRATION DATA

Thermistor Serial Number: 2

Power Conditioner Serial Number: 2

Thermocouple Readout Leeds & Northrup Millivolts	Thermistor Readout Fluke Meter Voltage	Temperature (°F)
-1.02	4.999	-5
- .83	4.67	2
- .7	4.46	7
- .50	4.12	14
- .39	3.90	18
- .28	3.65	22
- .11	3.37	28
+ .02	3.08	32.5
+ .18	2.82	38.5
.34	2.60	44
.46	2.40	48
.56	2.27	52
.70	2.05	57
.82	1.93	61
.94	1.77	65
1.06	1.63	69.5
1.2	1.46	74
1.32	1.35	79
1.48	1.24	84
1.74	1.08	93
1.92	1.01	99
2.09	.92	105
2.52	.72	120
2.3	.81	112
2.7	.66	126
2.85	.61	131
3.08	.54	139
3.26	.5	145
3.41	.46	150

temperature within $\pm 1.5^{\circ}\text{F}$. Since thruster performance is not particularly temperature sensitive, this resolution capability is more than adequate for monitoring capacitor case temperature during system operation.

2.3.3 Torques

During assembly of the system two cases were encountered for which no torque data was available. In one case this problem was encountered during installation of beryllium oxide washers. Since the vendor, Brush-Wellman, had no data on allowable torques that can be used in conjunction with their beryllium oxide washers, it was necessary to determine if the torque recommended by General Electric for installing their silicon controlled rectifier was acceptable with the hardware as delivered by General Electric. An exploratory installation test revealed that the torques applied to the hardware supplied by General Electric caused cracking of the beryllium oxide washers. To preclude damaging the washers during final installation, it was necessary to redesign the nut assembly of the SCR as supplied by General Electric. Torque tests were subsequently performed over a range of torques. These tests revealed that the redesigned nut assembly could be torqued to a desirable value of 20 in.-lb and subsequently removed without damaging the beryllium oxide washer.

In the second instance the vendor, Dearborne Electronics, recommended torque that can be applied to the studs of the energy storage capacitor, proved to provide insufficient electrical contact with the particular hardware to be used during final assembly. Consultation with the manufacturer and subsequent exploratory tests performed at Republic resolved this question without damaging any capacitors. These two critical torque values are presented in the final engineering drawings of the system.

2.3.4 Integration of the Power Conditioning Subassembly

Figure 2 shows the location of the power conditioning subsystem relative to the rear bulkhead. It is located exterior to the bulkhead and secured to it so that mechanical loads encountered during shock and vibration are well distributed over the remaining thruster system (see Figure 3). During later system testing it became necessary to remove the power conditioning subsystem as a unit. While this procedure is relatively simple, it is now believed that the number of steps involved could be considerably reduced by a minor redesign of the attachment hardware.

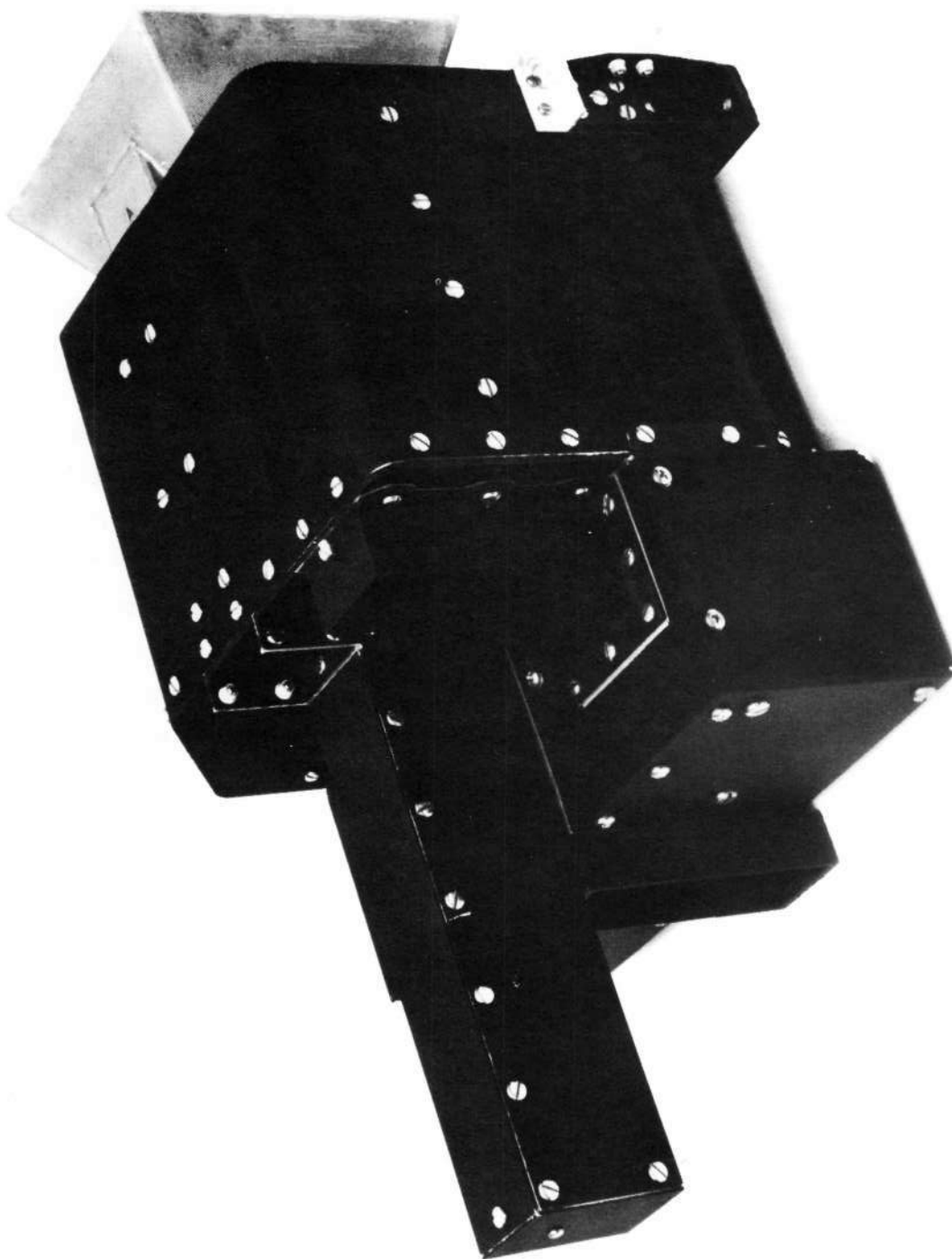


Figure 3. Microthruster System Showing Exterior Location of Integrated Power Conditioning Subsystem

Based upon the experience gained during the LES-6 flight system program, it was decided not to use any high voltage connectors in interfacing the power conditioner to the thruster in the present program. The technique incorporated was to hardwire the output leads of the power conditioner directly to the thruster terminals. This technique eliminated high voltage connectors and also bulkhead fittings (see Figure 2). An easily removable cover (PC145D1043-1, see Figure 3) readily exposes the output terminal field of the power conditioning subsystem and also the rear bulkhead through which the leads are passed to the interior of the thruster subassembly (see Figure 2 and particularly top right of Figure 4). This technique of electrically interfacing the two subsystems has proven itself vastly superior to the techniques used in earlier programs.

Another feature of the design readily allows electrical diagnostic leads to be passed into and out of the assembled system, if so desired, by merely removing a small cap (PC145D1016-1) located on the bulkhead just above the fuel track extension (see Figure 3).

2.4 System Weight, CG Location

The completely integrated system weight including propellant for more than 400 lb-sec of total impulse is 8.95 lb for Thruster A and 9.00 lb for System B. These two figures show the excellent reproducibility that can be had in building several units. This kind of reproducibility was also exhibited during the LES-6 flight thruster program. The 9 flight thrusters built in the latter program weighed as follows: 1379 gr, 1387 gr, 1387 gr, 1391.5 gr, 1390 gr, 1391 gr, 1390 gr, 1388.5 gr, 1388.3 gr.

The actual weights of the 8.95 and 9.00 lb of the SMS system are in excellent agreement and just slightly below the calculated value 9.13 lb of the final design presented in the Task 2 report (Ref. 2).

The location of the center of gravity of the completely integrated system (including propellant) was determined experimentally. Its location is presented in Figure 5. By locating the relatively heavy thruster capacitors as close as possible to the mounting plane (see Figure 2) and also having the power conditioning subsystem as close as possible to the mounting plane (also see Figure 2), it was possible to get the location of the CG below the geometric center of the thruster housing, or, as close as reasonably possible to the system mounting plane.

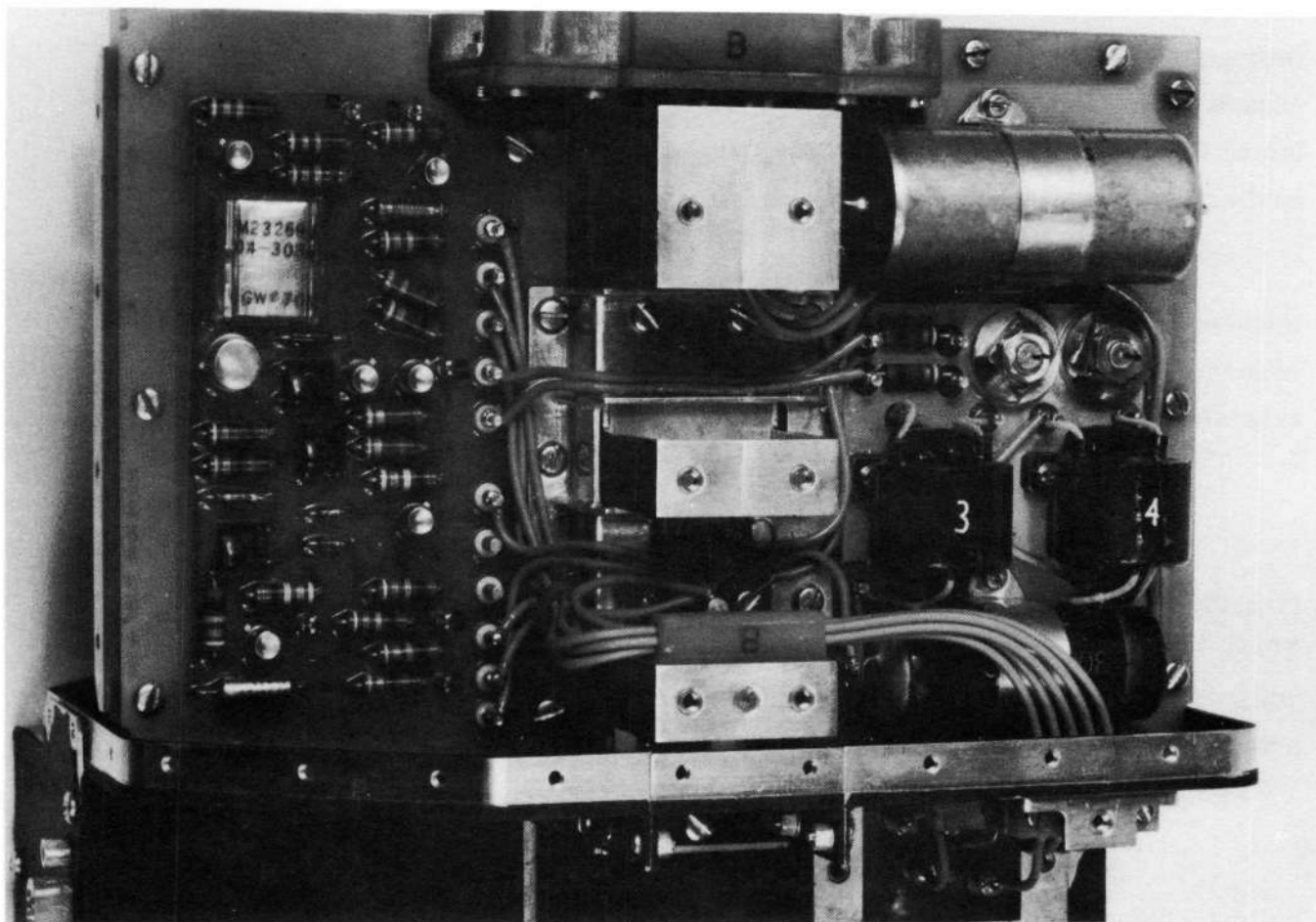


Figure 4. Thruster Electronics Subassembly

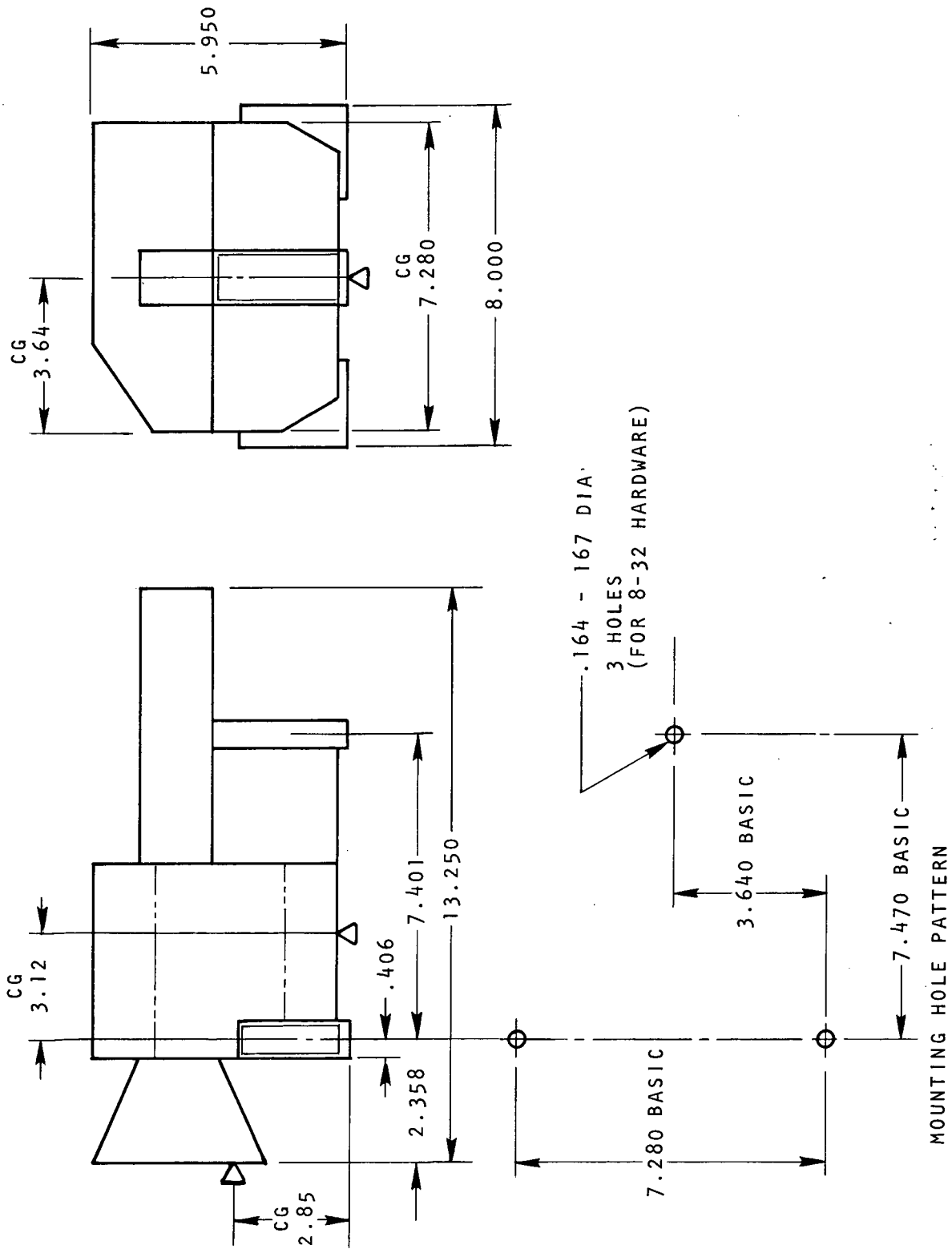


Figure 5. Location of CG and Mounting Holes

2.5 Mounting Hole Pattern, Thrust Axis Location

As indicated earlier, only three tie down points are required to mechanically integrate the complete propulsion system to one continuous mounting platform in the SMS spacecraft. The mounting hole pattern is shown in Figure 5.

The exact location of the thrust axis relative to the reference mounting base plate will be determined at Goddard Space Flight Center. A front coated mirror with a set of mutually perpendicular cross hairs on it is provided on the front face of the thruster to facilitate installation of the propulsion system such that the thrust axis is known relative to the spin axis of the spacecraft. The front coated mirror is located below the thruster nozzle as can be seen in Figure 6.

2.6 Connector Location

While system operation on the SMS spacecraft requires only one electrical connector, another connector was incorporated to facilitate laboratory diagnostic studies. Both of these connectors are located on the power conditioning subsystem and none of the pins on either connector carries a voltage higher than the 29.4 ± 2 volt supply voltage. The location of the two connectors on the power conditioning subsystem can be seen in Figure 7. One of these connectors, (the vertically mounted one in Figure 7), denoted as J-1, accommodates all primary input and return functions including telemetry. The other connector (the 9 pin horizontally mounted one in Figure 7), denoted as J-2 serves as a hardwire monitor for laboratory diagnostic purposes. The connector pin assignment of either connector is presented in Table 5.

The extreme simplicity in system integration and operation is seen from the connector pin requirements of the J-1 connector. Normal propulsion system operation can be carried out throughout the SMS 5 year mission life and under all spacecraft environmental conditions without the use of telemetry. Telemetry is provided merely for diagnostic purposes.

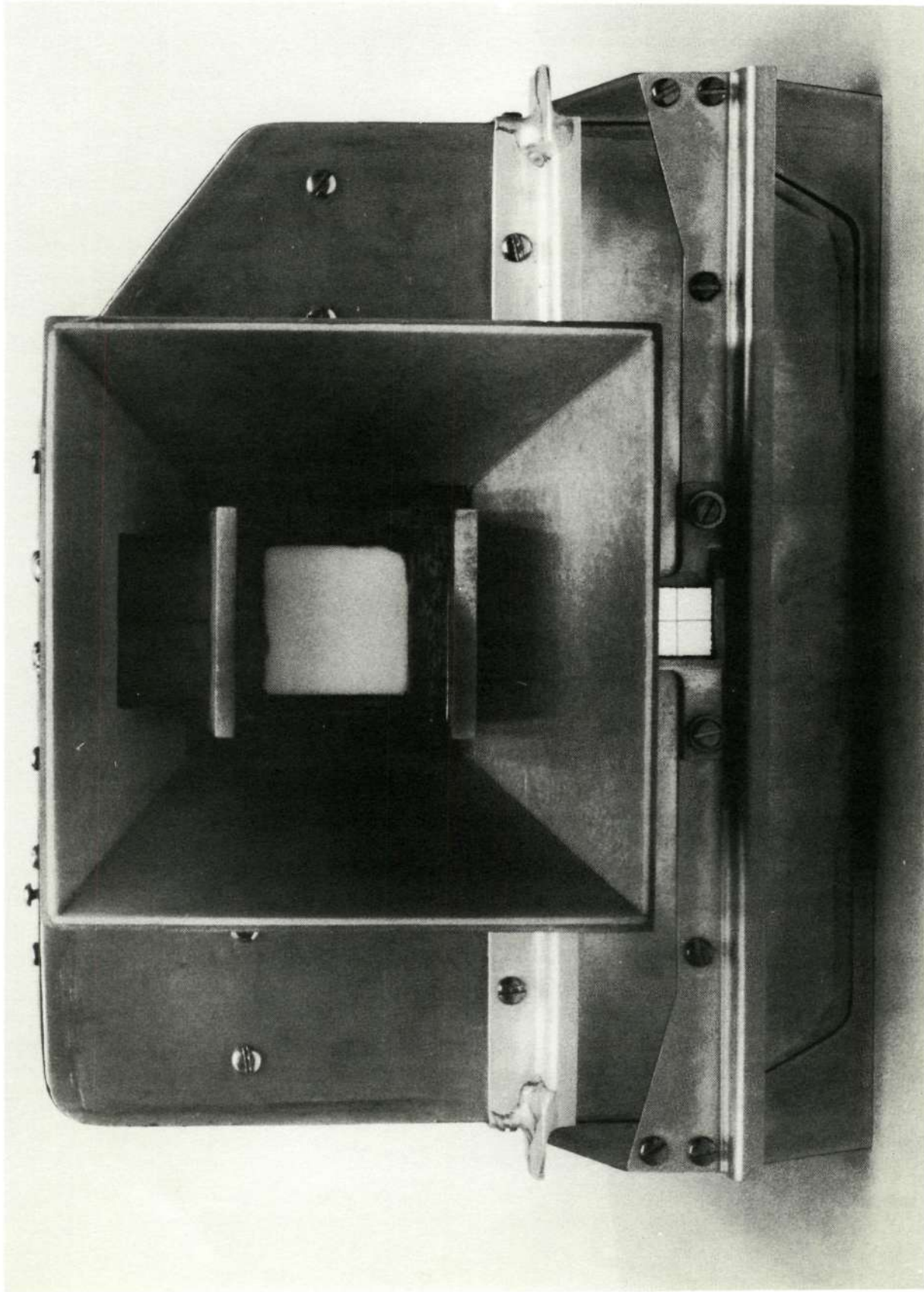


Figure 6. Front View of Propulsion System

Reproduced from
best available copy.

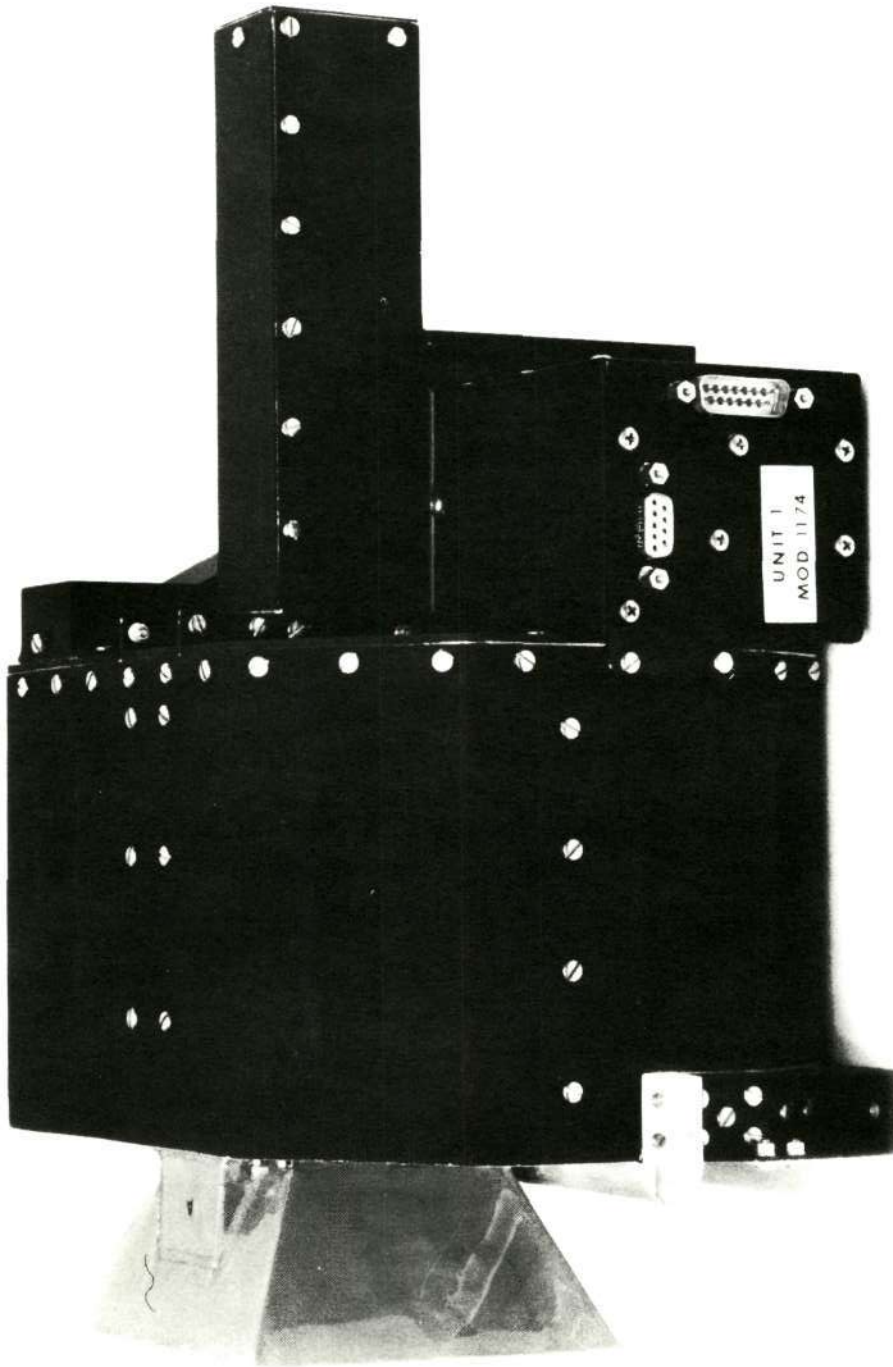


Figure 7. Side View of System Showing Connector Location

TABLE 5. CONNECTOR PIN ASSIGNMENT

Connector	Pin Number	Function	Classification
J-1	1 & 2	+29.4 Volts	Input
J-1	3 & 4	29.4 Volts Return	Input
J-1	5 & 6	Enable	Input
J-1	7 & 8	Fire Command	Input
J-1	9	Thrustor Temperature Telemetry	Output
J-1	10	1450 V Telemetry (0 to 5 volts)	Output
J-1	11	620 V Telemetry (0 to 5 volts)	Output
J-1	12	Enable Telemetry (0 to 5 volts)	Output
J-2	1	Power Return	Input or Output
J-2	2 thru 4	Not Used	
J-2	5	29.4 V	Output
J-2	6	Hold Time Monitor (for vendor purposes only)	Output
J-2	7	H. V. Monitor (0 to 5 volts)	Output
J-2	8	Fire Command	Output
J-2	9	Enable	Output
Redundancy is provided on input pins as shown above.			

3.0 SYSTEM OPERATION

3.1 General

Operation of the propulsion system is extremely simple. The system is mechanically mounted to a continuous base plate with 8-32 mounting hardware to interface to the 3-hole pattern shown in Figure 5. The external case of the thruster must be connected to the common ground tie point such that the total resistance between the case and the common ground is about 67 milliohms or less. Connector J-1 is connected to the propulsion system to provide the 29.4 ± 2 volt input power, the 28 ± 2 volt enable signal and the Fire Command Signal (see Table 5). For diagnostic purposes four telemetry output signals are also provided in the J-1 connector. After the system

has been evacuated to a pressure below 5×10^{-5} mm Hg for at least 4 hours, one can operate the system by following steps:

- a) Apply the 29.4 ± 2 VDC input power
- b) Apply the fire command signal at any desired pulse rate in the range 50 ppm to 110 ppm
- c) Apply the 28 ± 2 VDC enable signal

Power will be drawn by the system only after Step c) has been carried out. Depending upon the rate of the applied fire command signal, the first impulse bit will be provided in the range from 0.55 to 1.2 seconds after enabling the system by Step c) above. Removal of the 28 volt enable signal instantly shuts down the system without further power being drawn from the primary power source.

The propulsion system can provide either a) singular impulse bits; b) a train of n impulse bits, or c) operate steadily at a pulse frequency f . These three modes of operation will provide the following performance capability:

For Case a) An impulse bit (I_b) of about 25 micro-lb-sec

For Case b) A total impulse equal to the product of the number (n) of pulses in the train of pulses times the 25 micro-lb-sec impulse bit (I_b) amplitude of each pulse, i. e.,

$$I = n I_b$$

For Case c) An equivalent steady thrust level (T) of amplitude

$$T = f I_b$$

The total impulse in this latter case is equal to the product of the thrust level (T) times the total time of thrusting.

These three different modes of operation can be readily implemented by merely controlling the duration of application of the 28 ± 2 volt enable signal once the 29.4 ± 2 VDC power and fire command pulses are applied. In all cases the system will draw power only while the enable signal is applied.

Furthermore, in all three cases the specific impulse and thrust efficiency will be the same. The time average power drawn by the system, however, is strictly

a function of the pulse frequency of operation after being enabled by the 28 VDC signal. The power drawn by the system for various pulse frequencies is presented in Section 4.1.4.

3.2 On the Satellite

The 29.4 VDC power source and the fire command signals can be continuously impressed upon the system. They will be rejected by the system as long as the 28 ± 2 VDC enable signal is not applied to pins 5 and/or 6 of the J-1 connector. After application of the 28 VDC enable signal, the propulsion system will start generating impulse bits equal to the rate of the impressed pulse frequency (50 ppm to 110 ppm) of the fire command. The impulse bit will be accurately provided relative to the leading edge of the fire command signal. It is delayed precisely, however, by the delay pulse generator (PC145D1071) by about 6 millsec relative to the leading edge of the fire command signal. It is important to note that the system should not be activated during launch, i.e., not to apply the 28 VDC enable voltage during launch. It is preferable to outgas the system in orbit for at least 4 hours before enabling the system.

3.3 In the Laboratory

The system has extra features incorporated to increase laboratory diagnostic capability. Mounting the system in the laboratory is still by means of the 3-hole pattern shown in Figure 5. However, in the laboratory it is possible to treat the system case ground by either of two techniques:

- a) In the first approach the system can be bolted directly to a grounded platform by means of 8-32 hardware as in the SMS satellite. The number of interfaces located between the microthruster and the system common ground tie point should be kept at an absolute minimum so that a resistance measurement between the thruster case and the common tie point does not exceed about 67 milliohms.
- b) In the second approach the case of the microthruster can be mounted on an insulated platform. The case ground return to the common ground tie point is made by a single conductor attached to the case of the microthruster. The total resistance of this ground return lead should also be kept below about 67 milliohms.

In the laboratory one can also optionally connect the J-2 connector (see Table 5) besides the normally required J-1 connector. This additional connection will allow one to use the hardwire monitor capability of the J-2 connector.

3.4 System Shutdown

3.4.1 On a Spacecraft

Removal of the 28 ± 2 VDC enable signal to 0 ± 1.2 VDC from a 5000 ohm source impedance will shut down the system. The 29.4 VDC and the fire command signals can still be applied continuously to the thruster system since they will be rejected unless the 28 VDC enable signal is applied.

3.4.2 In a Vacuum Chamber

While the system is normally shut down by simply removing the 28 VDC enable signal it may be preferable to first remove the 29.4 VDC and then a few seconds later the 28 VDC enable and the fire command signal. This latter sequence will more rapidly remove any residual high voltage on the capacitors. If a normal satellite shut down procedure is followed, i.e., removal of the enable signal and, for laboratory studies, later the 29.4 VDC power and the fire command signal, then one should wait at least 10-15 minutes before venting the vacuum chamber to atmospheric pressure. This wait will allow the high voltage to bleed off to an acceptably low voltage before the vacuum chamber is vented. In any case, it is desirable to place a resistive short across the anode and cathode of the electrode nozzle before touching these.

3.5 Power Conditioning Subsystem Operation

Integration of the power conditioning subassembly to the thruster was presented in Section 2.3.3. This section will briefly describe operation of the power conditioner subassembly (details of the design may be found in Ref. 2).

The Power Conditioner receives input power at connector J-1. The input power is filtered by feed-through type and lumped LC filters. These filters also serve to keep any noise generated internally from getting out to the 29.4V power buss and source.

The unit contains an auxiliary power supply which furnishes + & - 12V power for internal use and 620V, +12V, +29.4V for external use. The auxiliary power supply is turned on by an internal enable switch which receives an enable signal from outside the unit via pins 5 and/or 6 of connector J-1 (see Table 5). In the absence of an enable signal, the entire power conditioner is off.

The subassembly receives external fire command pulses through pins 7 and/or 8 of connector J-1. These pulses are fed through the subassembly and also back out pin 8 of connector J-2 and also output terminal 3. The fire commands are used in the power conditioner to "condition" the delay generator. The delay generator commands the high voltage power converter "on" at such a time that the "hold time", or time that the output voltage on the external 8.0 μ f thruster energy storage capacitor is at 1450 volts, is maintained at this voltage between 5 and 50 milliseconds. The delay generator does this by sensing the actual "hold time" obtained, comparing this against an internal time standard, and using the difference by which actual hold time differs from ideal to control the amount of delay generated. This delay time is the time from discharge of the 8.0 μ f load capacitor (i. e., impulse bit generated) to the beginning of energy delivery to the same capacitor.

The comparator-regulator portion of the power conditioner serves to regulate the 1450 volt output at this level $\pm 1\%$. The coarse comparator senses that the 8.0 μ f capacitor actually gets "fired" upon receipt of each fire command pulse and "conditions" the delay generator to accommodate a misfiring.

Three telemetry amplifiers are incorporated whose inputs connect to various resistive voltage dividers and whose outputs represent scaled replicas of the enable signal, the value of the 620V output, and the value of 1450V output. An input for the thruster temperature telemetry amplifier is also provided. Its output is at pin 9 of connector J-1. All 4 telemetry amplifier outputs are taken out through feed-through type EMI filters.

The high voltage power converter furnishes the energy required to charge the 8.0 μ f thruster energy storage capacitor at a constant rate. It is capable of charging an 8.0 μ f $\pm 5\%$ capacitor from 0 to 1450 volts in 0.5 second ± 40 msec. Its associated comparator-regulator operates to control operation so as to regulate or hold

the output voltage at 1450 after it reaches that value. The charging is accomplished in such a manner that, during the 0.5 second charge time, input current from the 29.4 volt buss is nearly constant.

Performance data of this power conditioning subassembly is presented in Section 4.1.1. Figures 1, 2, 3 and 7 show the location of the power conditioning subsystem on the microthruster. Figure 8 shows the interior of the power conditioner.

4.0 TESTING CARRIED OUT

The testing that was performed during the Task 4 effort occurred at two levels: 1) subassembly tests, and 2) complete system testing. The subassembly testing was performed primarily to assure quality of the subassembly. The subassembly, or in-process tests, that were performed are presented in Table 2. Of the subassembly tests, the power conditioning unit represents a major subassembly and some further details of the tests performed on it are presented below. Details of the tests and results of the tests performed on the completely assembled propulsion system are also presented below.

4.1 Power Conditioning Test Data

4.1.1 By the Vendor

Both power conditioners (Unit #1 and Unit #2) were bench tested at Wilmore Electronics, Inc., prior to being shipped to Fairchild Republic for further testing and system integration. The following data was obtained at Wilmore:

Unit #1: With an 8 μ fd load capacitor across the high voltage output terminals and no fire commands imparted to the unit the steady state readings presented in Table 6 were obtained with a 29.4 volt input to the unit.

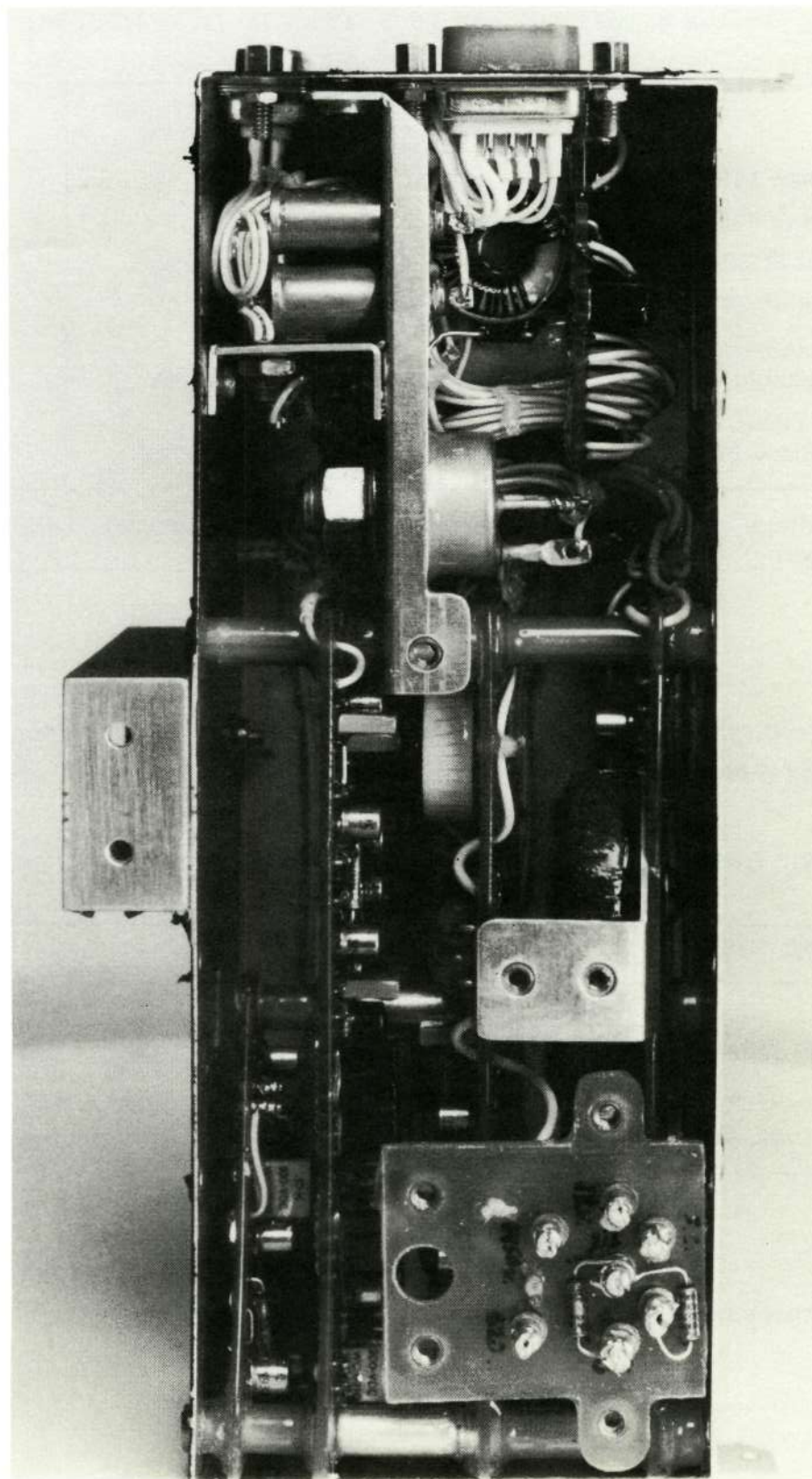


Figure 8. Interior View of Power Conditioning Subsystem

TABLE 6. STEADY STATE OUTPUT DATA -- UNIT NO. 1

	Cold Temp. -20 C	Room Temp. +23 C	Hot Temp. +60C
High Voltage 1450V	1449.1V	1451.5V	1454.3V
High Voltage 620V	628.6V	631.5V	637.4V
29V Output at 50 MA Load	29.2V	29.2V	29.2V
12V Output at 25 MA Load	12.0V	12.0V	12.0V
Enable Telemetry Output for 29.4V Enable Signal	4.4V	4.4V	4.4V
Thruster Temp. Telemetry Output for 0 Input	+29MV	+38MV	+45MV
All low voltage outputs above including telemetry were measured with 1000 ohm/ volt voltmeter.			

Under the same test conditions as stated above, the input buss voltage to the system was varied and the 620V and 1450V output voltages were again recorded as a function of the three temperatures indicated. Table 7 presents these results.

TABLE 7. OUTPUT DATA AS A FUNCTION OF INPUT VOLTAGE VARIATION

Input Voltage	620V Output			1450V Output		
	-20°C	23°C	60°C	-20°C	23°C	60°C
29.2V	624	628	633	1449	1451	1454
29.4V	628	632	637	1449	1451	1454
29.6V	633	636	642	1449	1451	1454

When a resistive load was switched across the 1450V output, the data presented in Table 8 was obtained at room temperature.

TABLE 8. DATA WITH RESISTIVE LOAD

	With 50K Load	With 100K Load
Output Voltage	950V	1370V
Output Current	18.75MA	13.55MA
Input Current From 29.4V Source	.790A	.832A
Efficiency	79.7%	81.9%
NOTE: The output current in Table 8 does not include current taken by a 10 Meg scope probe and 1000 ohm/v voltmeter on its 1.5KV F.S. range. These are considered in the above efficiency calculations.		

Each high voltage output was subsequently short circuited through an ammeter one at a time and input and output currents were measured. This data is presented in Table 9.

TABLE 9. SHORT CIRCUIT DATA

	-20C		+23C		+60C	
	620V	1450V	620V	1450V	620V	1450V
Output S. C. Current	6.25MA	67MA	6MA	70MA	5.9MA	65MA
Input Current	163MA	112MA	163MA	128MA	162MA	136MA
Auxiliary Power Supply Oscillator Frequency						
	6.8 KHz		7.0 KHz		7.1 KHz	

After the latter tests, the power conditioner was operated at different pulse frequencies determined by a pulse generator providing firing command signals at the input and using an SCR discharge circuit across the 8 μ fd load capacitor.

The SCR discharge circuit was synchronized to the input pulse frequency. Following data was obtained under these conditions:

Charge time to charge 8.2 μ f from 0 to 1450V.

-20C	+23C	+60C
525 M sec	493 M sec	476 M sec

Charge time to charge 2.0 μ f from 0 to 600V.

300 M sec	300 M sec	300 M sec
-----------	-----------	-----------

Time to add delay after abrupt change from maximum to minimum PRF.

21 sec	25 sec	28 sec
--------	--------	--------

Time to take off delay by making gradual change in PRF from minimum to maximum.

65 sec	60 sec	42 sec
--------	--------	--------

Minimum and Maximum extremes of hold time observed during a 5 minute interval, temperature order the same.

At fast PRF	16-15 M sec	16-28 M sec	15-27 M sec
At slow PRF	10-32 M sec	10-40 M sec	7-40 M sec

The telemetry circuitry was then calibrated under steady state conditions at room temperature. The telemetry readings were taken with a null-type voltmeter which does not load the circuit. The output Z of the telemetry outputs are approximately 500 ohms. The telemetry calibration data for the 1450 volt output and the 620V output as well as the high voltage hardwire monitor output on connector J-2 are presented in Table 10, respectively.

TABLE 10. TELEMETRY CALIBRATION DATA (STEADY STATE)

620V Telemetry Output at J1-11	Corresponding Value of the Voltage at 620V Output Terminal
0.078V	0.0V
1.702	245
2.763	406
3.435	511
3.977	594
4.225	631
1450V Telemetry Output at J1-10	Corresponding Value of the Voltage at 1450V Output Terminal
0.072	0.0
1.315	413
2.157	710
2.849	954
4.060	1380
4.186	1451
Output voltage at J2-7 (H. V. Monitor)	
4.162V for 1451 volts out	

The 1450 volt telemetry data may be expressed as

$$V_{1450} = 365.20V_{tel} - 77.7$$

Unit #2: With an 8 μ fd load capacitor across the high voltage output terminals and no fire commands imparted to the unit, the steady state readings presented in Table 11 were obtained with a 29.4 volt input to the unit.

TABLE 11. STEADY STATE OUTPUT DATA -- UNIT NO. 2

	Cold Temp. -20 C	Room Temp. +23 C	Hot Temp. +60C
High Voltage 1450V	1448.1V	1448.7V	1449.6V
High Voltage 620V	609.5V	612.5V	615.4V
29V Output at 50 MA Load	29.2V	29.2V	29.2V
12V Output at 25 MA Load	12.2V	12.2V	12.3V
Enable Telemetry Output for 29.4V Enable Signal	4.4V	4.4V	4.4V
Thruster Temp. Telemetry Output for 0 Input	+30MV	+40MV	+48MV
All low voltage outputs above including telemetry were measured with 1000 ohm/ volt voltmeter.			

Under the same test conditions as stated above, the input buss voltage to the system was varied and the 620V and 1450V output voltages were again recorded as a function of the three temperatures indicated. Table 12 presents these results.

TABLE 12. OUTPUT DATA AS A FUNCTION OF INPUT VOLTAGE VARIATION

Input Voltage	620V Output			1450V Output		
	-20°C	23°C	60°C	-20°C	23°C	60°C
29.2V	605	609	610	1448	1449	1450
29.4V	610	613	615	1448	1449	1450
29.6V	614	617	620	1448	1449	1450

When a resistive load was switched across the 1450V output, the data presented in Table 13 was obtained at room temperature.

TABLE 13. DATA WITH RESISTIVE LOAD

	With 50K Load	With 100K Load
Output Voltage	995V	1332V
Output Current	19.7MA	13.25MA
Input Current From 29.4V Source	.860A	.789A
Efficiency	80.3%	81.2%
NOTE: The output current in Table 13 does not include current taken by a 10 Meg scope probe and 1000 ohm/v voltmeter on its 1.5KV F. S. range. These are considered in the above efficiency calculations.		

Each high voltage output was subsequently short circuited through an ammeter one at a time and input and output currents were measured. This data is presented in Table 14.

TABLE 14. SHORT CIRCUIT DATA

	-20C		+23C		+60C	
	620V	1450V	620V	1450V	620V	1450V
Output S. C. Current	6.3MA	67MA	6.13MA	73MA	6.0MA	77MA
Input Current	172MA	110MA	164MA	130MA	172MA	150MA
Auxiliary Power Supply Oscillator Frequency						
	7.9 KHz		8.1 KHz		8.3 KHz	

After the latter tests, the power conditioner was operated at different pulse frequencies determined by a pulse generator providing firing command signals at the input and using an SCR discharge circuit across the 8 μ fd load capacitor.

The SCR discharge circuit was synchronized to the input pulse frequency. Following data was obtained under these conditions:

Charge time to charge 8.2 μ f from 0 to 1450V.

-20C	+23C	+60C
525 M sec	490 M sec	465 M sec

Charge time to charge 2.0 μ f from 0 to 600V.

300 M sec	300 M sec	300 M sec
-----------	-----------	-----------

Time to add delay after abrupt change from maximum to minimum PRF.

22 sec	27 sec	26 sec
--------	--------	--------

Time to take off delay by making gradual change in PRF from minimum to maximum.

70 sec	60 sec	50 sec
--------	--------	--------

Minimum and Maximum extremes of hold time observed during a 5 minute interval, temperature order the same.

At fast PRF	20-34 M sec	20-34 M sec	16-34 M sec
At slow PRF	18-38 M sec	10-40 M sec	8-40 M sec

The telemetry circuitry was then calibrated under steady state conditions at room temperature. The telemetry readings were taken with a mill-type voltmeter which does not load the circuit. The output Z of the telemetry outputs are approximately 500 ohms. The telemetry calibration data for the 1450 volt output and the 620V output as well as the high voltage hardwire monitor output on connector J-2 are presented in Table 15, respectively.

TABLE 15. TELEMETRY CALIBRATION DATA (STEADY STATE)

620V Telemetry Output at J1-11	Corresponding Value of the Voltage at 620V Output Terminal
0.046V	0.0V
1.651	242
2.695	402
3.372	508
3.965	596
4.065	610.6
1450V Telemetry Output at J1-10	Corresponding Value of the Voltage at 1450V Output Terminal
0.041	0.0
1.201	409
2.134	740
2.857	995
3.802	1332
4.124	1449
Output voltage at J2-7 (H. V. Monitor)	
4.121 V for 1449 volts out	

The 1450 volt telemetry data may be expressed as

$$V_{1450} = 356.281 V_{tel} - 20$$

4.1.2 Prior to Integration

Besides the tests that were described in Section 4.1.1, a series of bench tests were performed at Republic with a power conditioner test set in accordance to Fairchild Republic document PC145S8018. Besides measuring the steady state 620 volt and 1450 volt outputs for buss input voltage variations of 29.2, 29.4 and 29.6 volts, the steady state outputs were also recorded with the output of a noise generator on the input buss voltage. Under all test conditions it was found (as also noted in the data presented in Section 4.1.1) that the output voltages met specifications.

Regardless of the pulse repetition rate encountered in the SMS application (in the range 50 ppm to 110 ppm), the time required to charge the main thruster capacitor to 1450 volts should fall within the limit $460 \text{ msec} < T_{\text{charge}} < 540 \text{ msec}$. Furthermore, the "hold time", i.e., the duration that peak voltage (1450 volts) is applied should fall within the limits $5 \text{ msec} < T_{\text{hold}} < 50 \text{ msec}$.

Since a number of input fire command pulses are required in order for the power conditioning rate sensing circuit to change the hold time so that it is minimized for the particular pulse rate impressed, the time (in seconds) that elapse to reduce the "hold time" again to 55 msec as the input fire command pulse rate is increased was also recorded. Tables 16 and 17 present the three sets of data obtained for power conditioners numbers 1 and 2, respectively. The data presented in Tables 16 and 17 show that the charge time is indeed essentially a constant independent of the pulse rate. Furthermore, the application of peak voltage is also kept at an absolute minimum (i.e., within the limits $5 \text{ msec} < T_{\text{hold}} < 50 \text{ msec}$) for all pulse rates and also over the input buss voltage range $29.4 \pm 0.2 \text{ volts}$. These results are significant. They show that the proposed concept of reducing unnecessary DC life impressed upon the thruster capacitor has indeed been implemented. The significance of this feature was analyzed and discussed in the Task 1 report (Ref. 1). Briefly what has been accomplished is a significant reduction in voltage stress during the 5 year life of the SMS mission. This may be illustrated by an example: to deliver 400 lb-sec of total impulse it is necessary that the thruster deliver 16×10^6 pulses of $25 \times 10^{-6} \text{ lb-sec}$ amplitude. Thus over the 5 year life the total number of hours that the capacitor will be at peak voltage is thus $(16 \times 10^6) (T_{\text{hold}})/3600$. From the data presented in Tables 16 and 17 the largest T_{hold} is 40 msec. Thus, the worse case will be only 178 hours of DC life regardless of satellite spin rate. If this feature had not been incorporated, the applied stress could in the worse case be as much as 2920 hours. The stress level in the latter case is spin rate dependent with the worse case cited being encountered for a charge time designed to meet the highest spin rate of 110 ppm, but actually used at the 50 ppm spin rate.

4.1.3 Input Current Measurements

Measurements were made of the instantaneous circuit input to the completely integrated propulsion system during propulsion system performance acceptance tests. The input current was obtained by recording the voltage drop across

TABLE 16. CHARGE AND HOLD TIME FOR POWER CONDITIONER NO. 1

Spacecraft Power Voltage @ 29.2	Pulse Rate (PPM)	T Charge (Milliseconds)	T Hold (Milliseconds)	Time for T Hold = 55 MSec
	50	480	25	
	60	480	25	22.0
	70	480	25	15.0
	80	480	25	16.0
	90	485	25	17.0
	100	490	25	20.0
	110	490	25	17.5
Spacecraft Power Voltage @ 29.6				
	50	480	25	
	60	480	25	23.0
	70	485	25	12.5
	80	485	25	9.5
	90	485	25	16.0
	100	485	25	14.0
	110	485	25	16.5
Spacecraft Power Voltage @ 29.4				
	110	485	25	
	100	485	25	5
	90	485	25	5
	80	480	25	5.5
	70	480	25	6.0
	60	480	25	8.0
	50	480	25	7.5

TABLE 17. CHARGE AND HOLD TIME FOR POWER CONDITIONER NO. 2

Spacecraft Power Voltage @ 29.2	Pulse Rate (PPM)	T Charge (Milliseconds)	T Hold (Milliseconds)	Time for T Hold = 55 MSec
	50	480	40	21
	60	480	40	21
	70	460	40	13
	80	480	40	13
	90	470	30	15
	100	470	30	16
	110	470	30	11
Spacecraft Power Voltage @ 29.6				
	50	470	40	20
	60	480	30	21
	70	470	40	13
	80	470	40	12
	90	470	30	14
	100	470	25	22
	110	460	25	6
Spacecraft Power Voltage @ 29.4				
	110	460	25	
	100	470	30	10
	90	470	30	7
	80	470	30	7
	70	480	30	7
	60	460	30	8
	50	470	40	9

a calibrated current shunt in the 29.4 VDC input power line to the system. The instantaneous voltage variation across the shunt was displayed on an oscilloscope. Typical data of Thruster B are presented in Figures 9 through 12 for pulse rates of 108, 85.3, 70 and 53.5 ppm, respectively. For the shunt calibration of 50 mv/amp, Figures 9 through 12 present instantaneous input current variation with the current amplitude being equal to 0.4 amps/cm. A zero reference sweep line is presented in each photo for reference purposes. The data presented shows that the power conditioning subsystem operates essentially at constant current input conditions during capacitor charging. The time average current

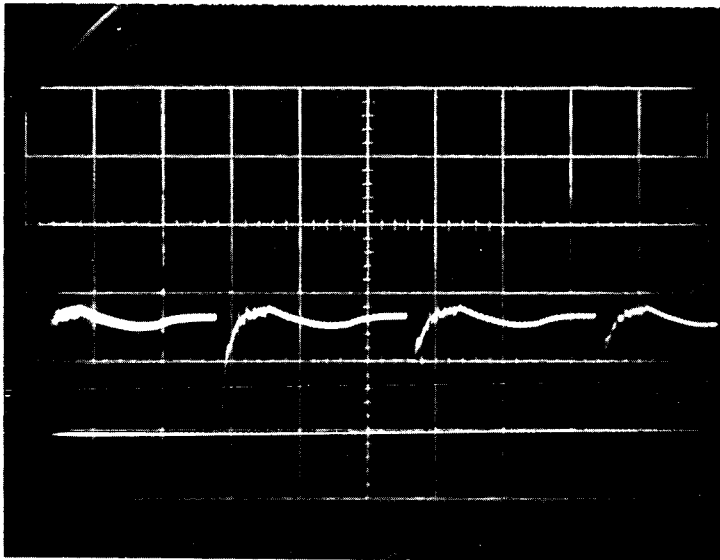
$$\bar{i} = \int_0^{\tau} i dt / \tau$$

(where τ is the period of a pulse) drawn by the entire propulsive system (including telemetry circuitry) during thruster operation is presented in Table 18.

TABLE 18. TIME AVERAGE CURRENT OF COMPLETE PROPULSION SYSTEM

Thruster	Pulse Rate (ppm)	Time Average Current (Amp)	Run
A	110	0.685	4
A	84.5	0.548	4
A	70.2	0.502	4
A	54.7	0.415	4
B	108	0.663	1
B	85.3	0.593	1
B	70	0.538	1
B	53.5	0.395	1

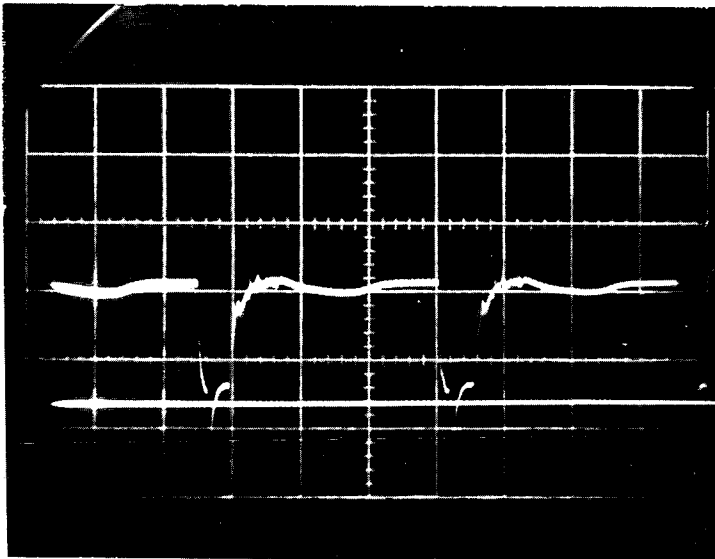
A close examination of Figures 9 through 12 reveals that instantaneous peak current is very nearly equal to current amplitude on the flat portion of the charge cycle.



0.2 sec/cm sweep
0.02 v/cm gain
50 mv/amp calib.

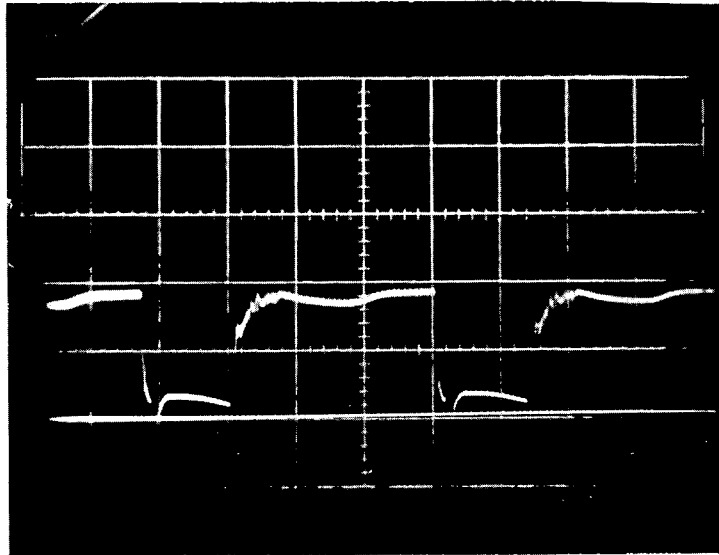
Reproduced from
best available copy.

Figure 9. Input Current at 108 PPM



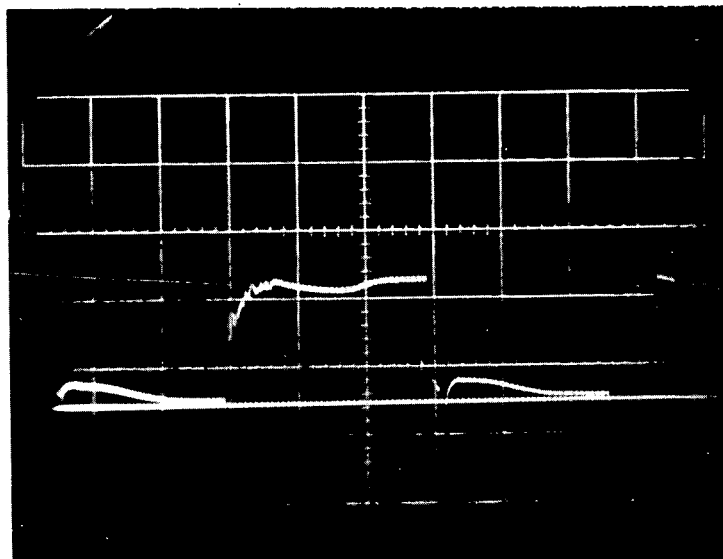
0.2 sec/cm sweep
0.02 v/cm gain
50 mv/amp calib.

Figure 10. Input Current at 85.3 PPM



0.2 sec/cm sweep
0.02 v/cm gain
50 mv/amp calib.

Figure 11. Input Current at 70 PPM



0.2 sec/cm sweep
0.02 v/cm gain
50 mv/amp calib.

Figure 12. Input Current at 53.5 PPM

The "turn-off" feature of capacitor charging that has been incorporated in the power conditioning design to prolong capacitor life can also be seen in Figures 9 through 12. Figure 9 shows that at 108 ppm as soon as the thruster is pulsed, the system will immediately start the next charge cycle. Figure 10 shows a short "off" time between pulses. The "off" time at 70 ppm (Figure 11) is longer yet and at 53.5 ppm one can see that the "off" time is almost comparable to the charge cycle time. Some idle current is drawn by the system during the "off" time between firing pulses while the system is activated by the 28 volt enable signal. Removal of the 28V enable signal completely shuts down the system with no current being drawn by the system.

4.1.4 Total Propulsion System Power Measurements

The thruster system whose data is shown in Figures 9 through 12 was operated with 29.4 volts input voltage. The power input of the system can readily be evaluated from the data presented in the latter figures. The time average power during thruster system operation is simply

$$\overline{P} = V_o \int_0^{\tau} i dt / \tau$$

with V_o the 29.4 volts applied and the remaining quantities as defined in Section 4.1.3. Table 19 presents the time average power used by the system during operation.

TABLE 19. TIME AVERAGE POWER OF COMPLETE PROPULSION SYSTEM

Thruster	Pulse Rate (ppm)	Time Average Power (watts)	Run
A	110	20.1	4
A	84.5	16.1	4
A	70.2	14.72	4
A	54.7	12.2	4
B	108	19.45	1
B	85.3	17.42	1
B	70	15.8	1
B	53.5	11.6	1

The data of Table 19 is presented in Figure 13. Besides the two sets of data of Table 19 several additional data points were available from prior runs (1 and 3) of System A. For reference purposes the higher specification power requirement is also presented.

Normally it is expected that the time average power (\bar{P}) should vary linearly with pulse rate (f) in accordance with the relation

$$\bar{P} = f E_d / \eta$$

where E_d is the discharge energy and η the power conditioning efficiency. The data presented in Figure 13 shows that the relation holds very nearly true for Thruster A run 4 over the entire range of pulse frequencies tested. It is suspected that the deviation from the linear relationship encountered during the other tests may be due to the power used between pulses before the charge cycle starts and also because the time at peak voltage is usually shorter at the 110 ppm rate than any other rate. The time average power of only the capacitor charge cycle has been found to be virtually independent of pulse rate as will be shown in Section 4.1.5.

4.1.5 Time Average Power of Charge Cycle

As stated in Section 4.1.4, the time average power of only the capacitor charge cycle portion of the system power curve was found to be essentially constant. The time average power averaged over the charge cycle is presented in Table 20. It can be seen that the departure of the average power over the charge cycle

TABLE 20. TIME AVERAGE POWER AVERAGED OVER
THE CAPACITOR CHARGE CYCLE

Thruster	System Pulse Rate (ppm)	Average Power Over Charge Cycle, Watts	Charge Cycle Duration (sec)	Run
B	108	19.45	0.55	1
B	85.3	20.3	0.60	1
B	70	19.9	0.60	1
B	53.5	20.3	0.60	1
Average of all readings		19.99		

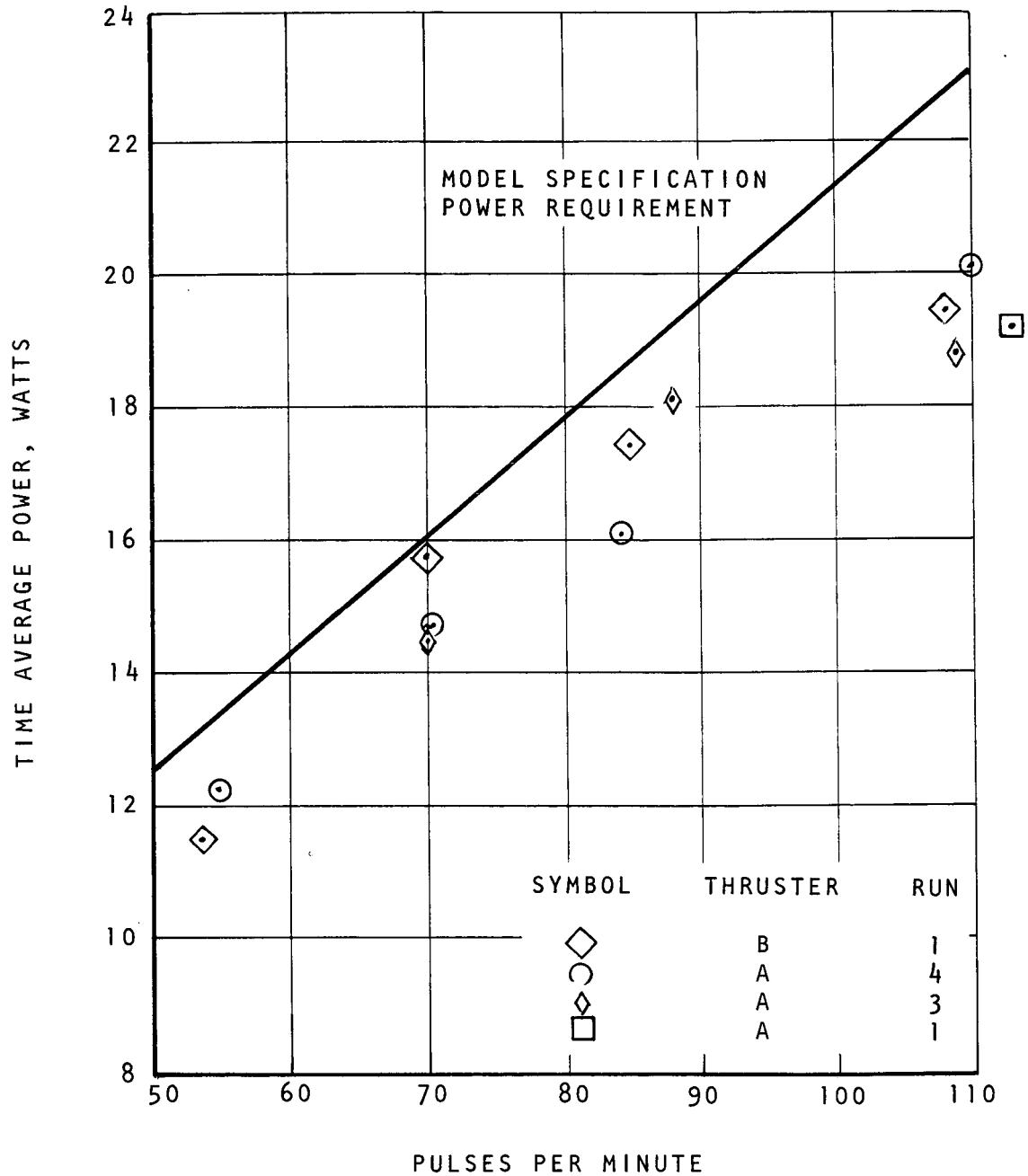


Figure 13. Time Average System Power Consumption

is within 3% of the mean value over the entire range of pulse rates. Thus the power required to charge the thruster capacitor during the charge cycle is essentially a constant independent of pulse rate. The magnitude of this power is of course completely governed by the design requirement that the power conditioner be capable of charging the capacitors for operation at the maximum pulse rate of 110 ppm. The unique feature of sensing the actual rate of the firing command signals and adjusting the hold time to be a minimum (i.e., within the limits $5 < t_{\text{hold}} < 50$ millsec) implies that the time average power of the system will always be lower than the charge cycle power (except at 110 ppm where both will be the same). This fact is verified by comparing the results presented in Tables 18 and 19.

The experimental data presented in Figures 9 through 12 shows that some idle current is drawn in between charge cycles. Thus, some power is consumed in between charge cycles as long as the system is activated by the 28V enable signal. If no idle power were required between charge cycles the "ideal" total system power required would equal

$$\overline{P}_{\text{ideal}} = \overline{P}_{\text{charge}} (\tau_c / \tau)$$

with τ_c / τ the ratio of charge cycle to total pulse cycle time. Table 21 presents a comparison between actual total system power and the "ideal" system power.

TABLE 21. COMPARISON OF ACTUAL TO IDEAL TOTAL SYSTEM POWER (THRUSTER B)

Pulse Rate (ppm)	Actual Power (watts)	Ideal System Power (watts)	Actual/Ideal
108	19.45	19.45	1
85.3	17.42	17.29	1.001
70	15.8	13.95	1.133
52.5	11.6	10.85	1.069

The data presented in Table 21 shows the largest departure of actual from ideal total power for Thruster B to occur at about 70 ppm. The reason for this larger than average departure is not known.

4.2 Performance Acceptance Tests

The complete propulsion system was mounted on a thrust balance in a vacuum chamber. The system was electrically isolated from ground and a separate ground return lead was connected between the thruster housing and the system common ground outside the vacuum chamber. A 29.4 VDC power supply was used for primary power. Another 28 VDC power supply was used to provide the 28 volt enable signal. A 50 millisecond long, 5 volt amplitude command fire signal was provided by the power conditioner test set. With the propulsion system in the vacuum chamber evacuated below 5×10^{-5} mm Hg for at least 4 hours, the system was activated by three steps: 1) applying the fire command signals at the desired pulse rate in the range 50 ppm to 110 ppm, 2) applying the 29.4 VDC primary power, and 3) applying the 28 VDC enable switch. The system was performance tested in accordance with Fairchild Republic document PC145S8026 Rev. B. During acceptance performance testing thrust data was taken three different times at pulse rates of 110 ppm, 90 ppm, 70 ppm and 50 ppm. The thrust balance was calibrated each time thrust data was taken. Telemetry data and system current input data was recorded while the propulsion system was operating at the four pulse rates.

Four separate performance acceptance tests were performed on Thruster 1 and one on Thruster 2. The tests performed are presented in Table 22. The first test

TABLE 22. PERFORMANCE ACCEPTANCE TESTS

Run No.	Log	Date	Thruster	Power Conditioner	Pulses of Test
1	146-1	6/21/71	1	1	14,690
2	146-2	6/26/72	1	2	1,615
3	146-3	6/27/72	1	2	16,243
4	146-4	7/21/72	1	1	18,130
1	147-1	7/26/72	2	2	18,105

(Log 146-1) had to be terminated after 14,690 discharges. The 1460 volt high voltage output of the power conditioner became inoperative because of the failure of a TX2N3821 FET in the power conditioner comparator circuit. Besides this failure, it was also

noted that an EMI filter in the 620 volt telemetry line was faulty. The vendor advised us that the EMI filter may have been accidentally damaged during final bench tests performed on an insulated bench while maintaining an ungrounded housing. Under such conditions the case may electrostatically float to a voltage in excess of the voltage rating of the EMI filter. The system functioned normal right up to failure with no signs of impending failure. Since the second power conditioner was available, it was integrated to the first thruster so that testing would be resumed with the shortest down time.

The second test (Log 146-2) was deliberately stopped after 1615 discharges because of improper flip-flop action of the thruster logic circuit. Replacing the ground return by a single ground wire whose total resistance measured 67 milliohms on a bridge resolved this matter. No data was taken during this second test. The third acceptance test (Log 146-3) was carried out and the system was operated at 110 ppm, 90 ppm and 70 ppm. Operation at 50 ppm was about to begin when the 1450 volt output of the second power conditioner was lost. Failure analysis revealed that the same FET that failed in the first power conditioner had again failed. The failed FET of the first tests was forwarded to GSFC for failure analysis. It has tentatively been concluded that the unit is from a lot which will exhibit a failure when subjected to even the slightest over voltage under the pulse mode of operation it is subjected to. Under normal operating conditions the FET is an acceptable unit.

Because of the two failures that were encountered, it was decided upon to replace the FET by units from another manufacturing lot. Furthermore, to preclude the possibility of transient over voltages reaching the FET, filter capacitors were placed in the +12.5 and -12.5 volt lines of the FET. Also, a bypass capacitor was placed between power conditioner ground and the case of the power conditioner. The thruster electronics circuitry was modified by inserting an inductive choke between the cathode of the thruster and thruster common ground. Both systems were subsequently performance acceptance tested (Log 146-4 and Log 147-1) with these modifications without further incidence. Thruster performance data was taken during four of the five tests performed. The results are presented in Section 4.2.1. Measurements of system current and power during these tests were presented in Sections 4.1.3 through 4.1.5.

4.2.1 Thrust and Impulse Bit Data

The thrust and impulse bit data that was obtained during the performance acceptance tests tabulated in Table 22, are presented in Tables 23, 24 and 25. Table 23 presents the data of Log 146-1 and 146-2. Tables 24 and 25 present the final acceptance test data of the first and second propulsion system, respectively.

The specific impulse was also established during these tests. For the last three tests it was 620 sec, 612 sec, and 642 sec, respectively. These values exceed the conservative value of 450 sec assumed in the propellant system design. The 400 lb-sec total impulse capability of the propellant system has, therefore also been met and exceeded.

An examination of the thruster performance data presented shows that the design impulse bit amplitude rating of 25 micro lb-sec has indeed been met and even slightly exceeded. The test average impulse bit amplitudes of 34.92 and 34.56 micro lb-sec are in extremely close agreement with each other. The test average impulse bit amplitudes of either propulsion system over the range of pulse rates examined show an essentially constant value. The departure of the average impulse bit at any pulse rate from the overall test average is presented in Table 26. This shows the impulse bit amplitude to be essentially constant independent of pulse rate.

It is interesting to note that the impulse bit amplitude at the highest pulse rate for both systems is slightly below the test average value. This observation suggested that perhaps the applied voltage just prior to a discharge is slightly lower than the value applied at lower pulse rates. Originally it was thought that the 1450 Volt telemetry data also supported this hypothesis. However, a high voltage probe applied directly to the power conditioner output showed that the 1450 volt output of the power conditioner is indeed within design specifications. This latter data is presented in Section 4.2.3.

4.2.2 Total Impulse Capability

The total impulse capability of the propulsion system is designed to be at least 400 lb-sec. Two uninterrupted performance tests were reported earlier in the program (Ref. 1) with prototype thrusters demonstrating by life tests a total impulse capability with available propellant of 380.8 lb-sec (Log 126X-7) and 385.5 lb-sec (Log 129-3). These earlier figures demonstrated 95% of the design life. During the

TABLE 23. THRUST AND IMPULSE BIT DATA LOG 146-1, 146-3

a) <u>Log 146-1</u>				
Actual Pulse Rate (ppm)	Measured Thrust (micro lb)	Measured Impulse Bit (micro lb-sec)	Average Impulse Bit* (micro lb-sec)	Test Average Impulse Bit (micro lb-sec)
111	46.5	25.1	26.4	26.4
	48.6	26.2		
	51.8	28.0		
(90)	47.5			
b) <u>Log 146-3</u>				
104.4	48	27.6	29.6	32.6
	53.2	30.6		
	53.0	30.4		
83.1	46.9	33.8	34.2	
	46.3	33.4		
	49.0	35.4		
68.3	40.4	35.5	34.1	
	37.2	32.7		
* For particular pulse rate				

TABLE 24. ACCEPTANCE THRUST AND IMPULSE BIT DATA
SYSTEM 1 (LOG 146-4)

Actual Pulse Rate (ppm)	Measured Thrust (micro lb)	Measured Impulse Bit (micro lb-sec)	Average Impulse Bit* (micro lb-sec)	Test Average Impulse Bit (micro lb-sec)
104.2	54.33	31.30	32.68	34.92
	59.16	34.08		
	56.70	32.66		
82.4	49.97	37.59	35.82	
	51.65	37.59		
	46.05	33.52		
67.0	40.82	36.58	36.91	
	40.20	36.02		
	42.57	38.14		
52.1	33.19	38.19	37.61	
	32.57	37.48		
	32.30	37.17		

* For particular pulse rate

**TABLE 25. ACCEPTANCE THRUST AND IMPULSE BIT DATA
SYSTEM 2 (LOG 147-1)**

Actual Pulse Rate (ppm)	Measured Thrust (micro lb-sec)	Measured Impulse Bit (micro lb-sec)	Average Impulse Bit* (micro lb-sec)	Test Average Impulse Bit (micro lb-sec)
104.9	51.29	29.34	30.58	34.56
	54.73	31.31		
	54.36	31.10		
82.2	51.27	37.42	36.28	
	48.26	35.23		
	49.58	36.19		
67.4	38.37	34.14	34.24	
	37.61	33.46		
	39.47	35.11		
52.1	32.25	37.11	37.16	
	33.26	38.28		
	31.36	36.09		

* For particular pulse rate

TABLE 26. IMPULSE BIT AMPLITUDE VARIATION

Pulse Rate (ppm)	<u>Average Impulse Bit for ppm</u> <u>Test Average Impulse Bit</u>
System 1	
104.2	0.936
82.4	1.026
67.0	1.057
52.1	1.077
System 2	
104.9	0.884
82.2	1.049
67.4	0.991
52.1	1.075

Task 4 effort it was not required that the total impulse capability be again verified by test at Fairchild Republic. Such testing will be performed at Goddard Space Flight Center. However, based upon the test data that was generated during the performance acceptance tests during Task 4, one can calculate the total impulse capability of the system with the available usable propellant. The overall test average specific impulse of the two final acceptance tests (Log 146-4 and 174-1) were 612 and 642 sec, respectively. The total propellant weight initially installed in Thrusters A and B (Log 146-1 and 147-1) were 445.1928 gr and 446.1406 gr, respectively. Since a small length of the Teflon propellant rod is used to support the Negator spring and to guide the propellant into the nozzle, about 22 gr of the propellant cannot be used in a life test. Subtracting this quantity of propellant from the initial propellant weights, and using the specific impulse values measured, one finds a total impulse capability of 570 lb-sec for Thruster A and 600 lb-sec for Thruster B. These values meet and exceed the 400 lb-sec minimum requirement.

4.2.3 Measured High Voltage Output

The telemetry data of the 1460 volt output (Pin J1-10) under pulsing conditions suggests that the voltage on the capacitor at the instant of discharge is lower than the actual value. For example, during one of the tests following data was noted:

<u>PPM</u>	<u>Capacitor Voltage</u>
110	1390
90	1414
70	1444

The apparent lower telemetry high voltage reading has not been explained. That the power conditioner is actually supplying the correct voltage to the energy storage capacitor was measured during actual system operation under acceptance test conditions. A Tektronix high voltage probe was used to record the actual high voltage output provided to the thruster capacitor under vacuum operating conditions. Figures 14 through 17 present the latter data. In all cases, it is seen that the voltage actually supplied to the thruster capacitor is 1430 volts regardless of pulse rate. Thus, the amplitude is supplied correctly. It is interesting to note, however, that the "hold-time" at the highest

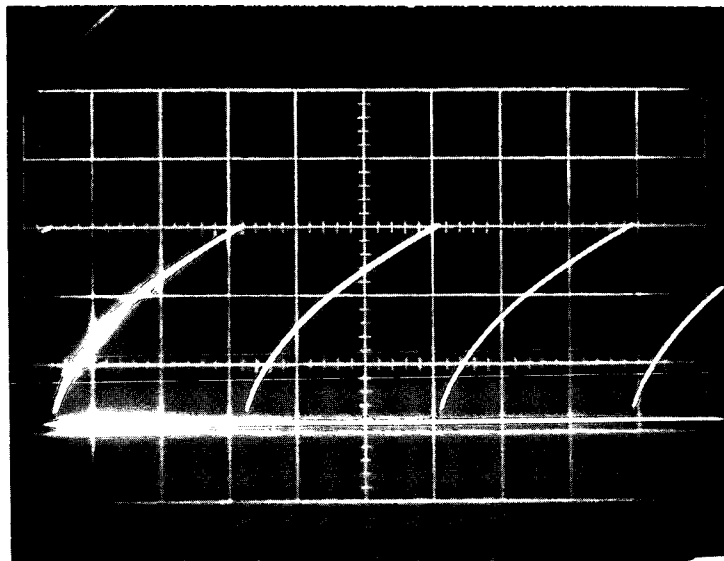


Figure 14. High Voltage Output at 104.5 PPM

Reproduced from
best available copy.

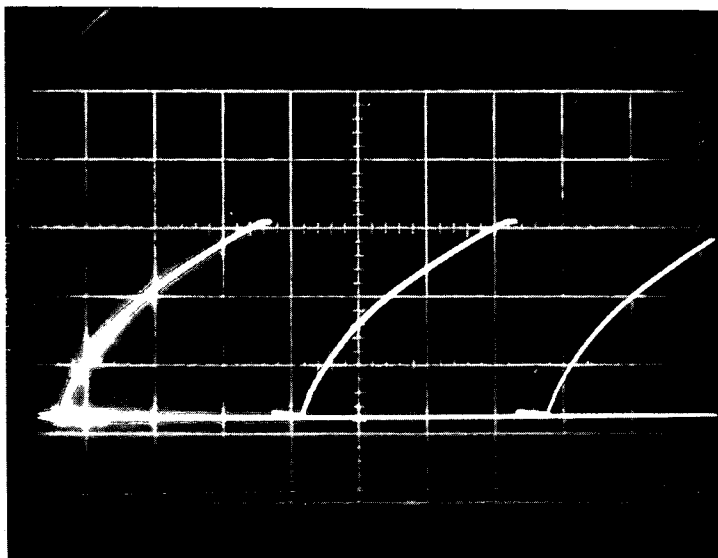


Figure 15. High Voltage Output at 83 PPM

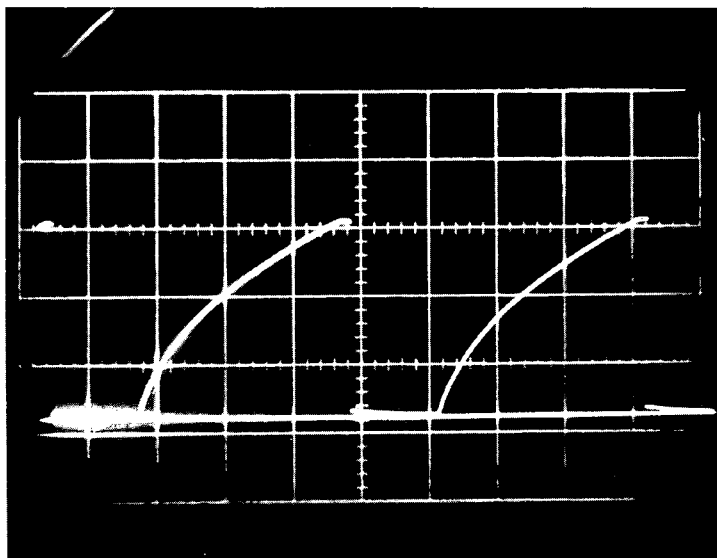


Figure 16. High Voltage Output at 69 PPM

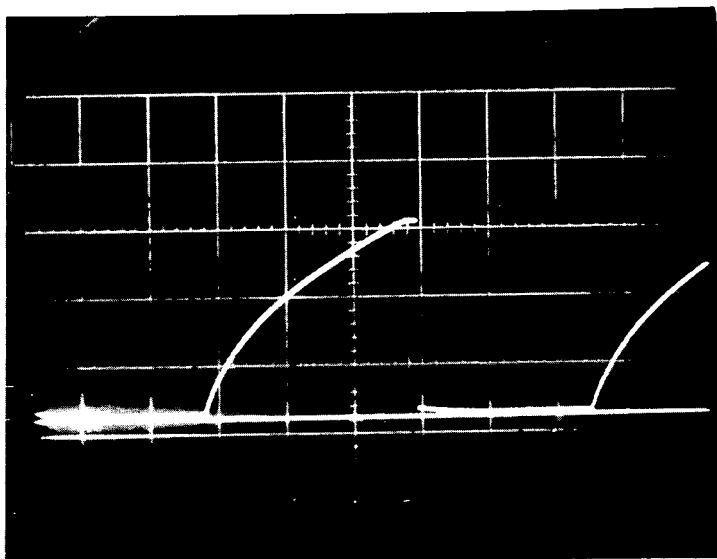


Figure 17. High Voltage Output at 53.8 PPM

pulse rate (see Figure 14) is virtually nonexistent. The voltage applied, however, is at the correct amplitude at the instant of discharge. This data shows that care must be exercised in performing diagnostic calculations using the high voltage telemetry data.

5.0 FINAL REMARKS

The results obtained during the Task 4 effort have shown that the flight proven LES-6 solid propellant system concept could be scaled up to meet the SMS requirements. The propulsion performance demonstrated met contract requirements as had been predicted from available empirical scaling relations governing such thrusters. The concept of reducing the DC voltage stress on the thruster capacitor was implemented and reduced the applied stress from a possible 2920 hours to about 178 hours. Experimental data has not yet been generated verifying that this reduction in voltage stress actually increases capacitor life. Such a verification would involve testing over and above contract requirements. Further testing of the flight prototype propulsion systems in addition to the tests performed at Fairchild Republic will be carried out at Goddard Space Flight Center.

While the overall effort has been successful in demonstrating that the SMS mission requirements can be met, a number of design improvements discussed in the report could be made to simplify fabrication and assembly of future systems. It is even possible to increase the thrust/power ratio of future systems by using a V-shaped propellant instead of a breech-fed propellant. However, even without such improvements, the two flight prototype systems that were assembled and tested met all expectations and demonstrate the readiness of the pulsed plasma propulsion system for the SMS application.

6.0 REFERENCES

1. "Task 1 - Design Analysis Report, Pulsed Plasma Solid Propellant Microthruster for the Synchronous Meteorological Satellite," Edited by W.J. Guman, Interim Report on Contract NAS5-11494, PCD-71-7, PC145R8000, FRD4070, Fairchild Industries, Fairchild Republic Division, Farmingdale, New York, December 1971.
2. "Task 2 - Flight Prototype System Design Report, Pulsed Plasma Solid Propellant Microthruster for the Synchronous Meteorological Satellite," Edited by W.J. Guman, Interim Report on Contract NAS5-11494, FRD 4082, Fairchild Industries, Fairchild Republic Division, Farmingdale, New York, April 1972.
3. Guman, W., Nathanson, D., Pulsed Plasma Microthruster System for Synchronous Orbit Satellite, J. Spacecraft and Rockets, Vol. 7, No. 4, April 1970 p. 409/415.